LMO3 Interacts with Neuronal Transcription Factor, HEN2, and Acts as an Oncogene in Neuroblastoma

Mineyoshi Aoyama,[1] Toshinori Ozaki,[1] Hiroyuki Inuzuka,[1] Daihachiro Tomotsune,[3] Junko Hirato,[4] Yoshiaki Okamoto,[1] Hisashi Tokita,[2] Miki Ohira,[1] and Akira Nakagawara[1]

Divisions of [1]Biochemistry and [2]Animal Science, Chiba Cancer Center Research Institute; [3]Center for Functional Genomics, Hisamitsu Pharmaceutical Co., Inc., Chiba, Japan and [4]Department of Pathology, Gunma University School of Medicine, Gunma, Japan

Abstract

LIM-only proteins (LMO), which consist of LMO1, LMO2, LMO3, and LMO4, are involved in cell fate determination and differentiation during embryonic development. Accumulating evidence suggests that LMO1 and LMO2 act as oncogenic proteins in T-cell acute lymphoblastic leukemia, whereas LMO4 has recently been implicated in the genesis of breast cancer. However, little is known about the role of LMO3 in either tumorigenesis or development. In the present study, we have identified *LMO3* and *HEN2*, which encodes a neuronal basic helix-loop-helix protein, as genes whose expression levels were higher in unfavorable neuroblastomas compared with those of favorable tumors. Immunoprecipitation and immunostaining experiments showed that LMO3 was associated with HEN2 in mammalian cell nucleus. Human neuroblastoma SH-SY5Y cells stably overexpressing LMO3 showed a marked increase in cell growth, a promotion of colony formation in soft agar medium, and a rapid tumor growth in nude mice compared with the control transfectants. More importantly, the increased expression of LMO3 and HEN2 was significantly associated with a poor prognosis in 87 primary neuroblastomas. These results suggest that the deregulated expression of neuronal-specific LMO3 and HEN2 contributes to the genesis and progression of human neuroblastoma in a lineage-specific manner. (Cancer Res 2005; 65(11): 4587-97)

Introduction

The LIM domain–containing proteins are important regulators in determining cell fate and controlling cell growth and differentiation during embryonic development (1). The LIM domain is a highly conserved cysteine-rich zinc finger–like motif found in a variety of nuclear and cytoplasmic proteins and acts as a docking site for the assembly of multiprotein complexes (2–4). However, the precise role of the LIM domain is still unclear. Several distinct subgroups of the LIM domain–containing proteins are defined and some of them also possess a functionally divergent domain, including a DNA-binding homeodomain or a protein kinase domain (1, 2).

The LIM-only proteins (LMO) are one of the families of the LIM domain–containing proteins and possess only two tandem LIM domains. They consist of four members, including LMO1, LMO2, LMO3, and LMO4 (2, 4). *LMO1* and *LMO2* have been identified as the genes that are activated in human acute T-cell leukemia (T-cell ALL) by tumor-specific chromosomal translocations (4). Transgenic mice overexpressing LMO1 or LMO2 developed immature and aggressive T-cell leukemia, suggesting that these proteins act as T-cell oncoproteins (5–7). On the other hand, LMO4 has been identified as a nuclear protein that interacts with the adaptor protein Ldb1 (8). It has been shown recently that LMO4 is highly expressed in primary human breast cancers, and overexpression of LMO4 inhibits differentiation of mammary epithelial cells, suggesting that deregulated expression of LMO4 contributes to the breast carcinogenesis (9). LMO4 has also been reported to be associated with BRCA1 to repress its transcriptional activity (10). Thus, LMO1, LMO2, and LMO4 have been implicated in tumorigenesis. However, to date, little is known about the oncogenic function of LMO3, which has been discovered based on sequence homology with LMO1 (11).

The nuclear LMO proteins, which lack intrinsic DNA-binding activity, have been considered to be involved in transcriptional regulation (2), raising a possibility that they alter the transcription of target genes by forming a complex with other transcription factors with DNA-binding activity. Indeed, in T-cell acute lymphoblastic leukemia in children, a basic helix-loop-helix transcription factor, TAL1, is physically associated with LMO1 or LMO2 and enhances their oncogenic activities (12, 13). Interestingly, the neuronal-specific basic helix-loop-helix transcription factors, HEN1 and HEN2, were identified based on cross-hybridization with TAL1 (14, 15). Their expression was restricted to the developing nervous system and a human neuroblastoma cell line. However, the role of HEN1 and HEN2 in tumorigenesis has long been elusive.

Neuroblastoma is one of the most common childhood cancers and is originated from sympathoadrenal lineage of the neural crest (16). It is clinically and cytogenetically divided into two major subgroups with favorable and unfavorable prognosis (17). The recent molecular and cellular analyses have revealed that amplification of *MYCN* and *DDX1* as well as loss of heterozygosity at the region of chromosome 1p36 are strongly associated with a poor outcome, whereas high levels of expression of the neurotrophin receptors *TrkA*, *CD44*, and *Fyn*, are well correlated with favorable prognosis (16–23). However, we still do not know many other genes that play important roles in the genesis and progression of neuroblastoma. To identify the other genes closely involved in neuroblastoma, we have constructed several cDNA libraries from different subsets of neuroblastoma and randomly cloned 4,200 genes (24). Screening of the genes differentially expressed between favorable and unfavorable subsets of the tumor has identified *Nbla3267* as one of the genes expressed at higher levels in unfavorable than favorable neuroblastomas (25).

In the present study, we found that *Nbla3267* encoded the human LMO, LMO3, and that high expression of *LMO3* as well as *HEN2* was strongly associated with a poor prognosis of neuroblastoma. Furthermore, LMO3 interacted with HEN2 in mammalian

Requests for reprints: Akira Nakagawara, Division of Biochemistry, Chiba Cancer Center Research Institute, 666-2 Nitona, Chuoh-ku, Chiba 260-8717, Japan. Phone: 81-43-264-5431; Fax: 81-43-265-4459; E-mail: akiranak@chiba-cc.jp.

cell nucleus, and enforced expression of LMO3 in human neuroblastoma-derived cell line SH-SY5Y markedly enhanced tumor growth in nude mice, supporting the oncogenic role of LMO3 in neuroblastoma.

Materials and Methods

Patient population. The RNA samples obtained from 87 patients with neuroblastoma were subjected to semiquantitative and quantitative real-time reverse transcription-PCR (RT-PCR) analyses. All patients were diagnosed clinically as well as pathologically and tested for DNA ploidy, MYCN amplification, and TrkA expression. Tumors were staged according to the International Neuroblastoma Staging System criteria (26). Thirty-four patients were stage I, 14 were stage II, 8 were stage III, 26 were stage IV, and 5 were stage IVS. Stages I, II, and IVS were considered as favorable and stages III and IV as unfavorable. The patients were treated following the protocols proposed by the Japanese Infantile Neuroblastoma Cooperative Study (27) and the Study Group of Japan for Treatment of Advanced Neuroblastoma (28). The clinical follow-up ranged from 4 to 58 months, with a median of 36 months. We have a precise list of patient characteristics, including age, stage, and clinical follow-up time, and this list will be provided upon request.

Cloning of human *LMO3*, *HEN1*, and *HEN2*. To obtain a complete human *LMO3* cDNA, a cDNA library derived from human fetal brain (Stratagene, La Jolla, CA) was screened with a ^{32}P-labeled *Nbla3267* cDNA. Plaques showing positive signals were picked up and rescreened twice. To construct the expression plasmid for hemagglutinin (HA)–tagged LMO3-A, the cDNA fragment encoding the entire LMO3-A protein was amplified by PCR from the phage clone as a template using the primers designed to add a synthetic linker encoding the HA epitope on the NH_2-terminal side of LMO3-A (forward 5′-GGTACCATGGCTTACCCATACGATGTTCCAGATTACGCTAGCCTCTCAGTCCAGCCAGACAC-3′ and reverse 5′-TCAGATATCATTAGATCAGCGAACCTGGG-3′). The PCR product was digested with *Kpn*I and *Eco*RV and subcloned into the identical restriction sites of pcDNA3 expression plasmid to give pcDNA3-HA-LMO3-A. cDNA encoding human HEN1 (amino acid residues 1-133) or HEN2 (amino acid residues 1-135) was generated by reverse transcribing total RNA isolated from neuroblastoma cell line, IMR32, using a forward primer (5′-AAGGAATTCATGCTCAACTCAGACACCATG-3′) and a reverse primer (5′-ATAAGAATGCGGCCGCTCAGACGT-3′) for HEN1 and a forward primer (5′-AAGGAATTCATGCTGAGTCCGGACCAAGCA-3′) and a reverse primer (5′-ATAAGAATGCGGCCGCCTACACGTCCAGGACGTGGTT-3′) for HEN2. The amplified PCR products were digested with *Eco*RI and *Not*I and subcloned into the identical restriction sites of pcDNA3-FLAG expression plasmid to give pcDNA-FLAG-HEN1 and pcDNA3-FLAG-HEN2.

Generation of a polyclonal anti-LMO3 antibody. The polyclonal anti-LMO3 and anti-HEN2 antibodies were raised against a peptide "Cys" plus containing the amino acid sequence between positions 127 and 145 of LMO3 and the amino acid sequence between positions 1 and 19 of HEN2, respectively. The peptides and the polyclonal antibodies were produced by Biologica Co. (Nagoya, Japan).

Cell culture and transfection. Human neuroblastoma (SK-N-AS, SH-SY5Y, NB69, OAN, SK-N-BE, NGP, NLF, IMR32, NB1, and KP-N-NS), ALL (RPMI, KOPT, HSB, and MOLT), osteosarcoma (OST, SAOS-2, and U2OS), rhabdomyosarcoma (RMS-MK), colon cancer (COLO-320), breast cancer (MCF-7 and MDA-MB-453), melanoma (G361, G32TG, and A875), thyroid cancer (TTC11), small cell lung carcinoma (H1299), and cervical cancer (HeLa) cell lines and COS7 cells were maintained in RPMI 1640 or DMEM supplemented with 10% heat-inactivated fetal bovine serum (FBS), 100 IU/mL penicillin, and 100 μg/mL streptomycin at 37°C in an atmosphere of 5% CO_2 in the air. For transient transfection, COS7 cells were transfected with the indicated expression plasmids using FuGene 6 transfection reagent as recommended by the manufacturer (Roche Molecular Biochemicals, Mannheim, Germany). Stable transfections of SH-SY5Y cells were done with the empty plasmid (pcDNA3, Invitrogen, Carlsbad, CA) or with the expression plasmid for FLAG-tagged LMO3-A using Lipofect-AMINE Plus transfection reagent according to the manufacturer's instructions (Invitrogen). The transfected cells were cultured in the presence of G418 at a final concentration of 400 μg/mL (Sigma Chemical Co., St. Louis, MO). Thereafter, the selection medium was replaced every 3 days. Three weeks after the selection in G418, drug-resistant clones were isolated and allowed to proliferate in medium containing G418.

Reverse transcription-PCR analysis. Total RNA was prepared from cultured cells and human tissues by using Trizol reagent (Life Technologies, Grand Island, NY) or the RNeasy Mini kit (Qiagen, Valencia, CA). Reverse transcription was carried out using random primers and SuperScript II (Invitrogen). Following the reverse transcription, the resultant cDNA was subjected to PCR-based amplification. Oligonucleotides used to amplify *LMO3-A*, *LMO3-B*, *LMO1*, *LMO2*, *LMO4*, *Ldb1*, *Ldb2*, *TAL1*, *HEN1*, *HEN2*, and glyceraldehyde-3-phosphate dehydrogenase (*GAPDH*) mRNAs were as follows: *LMO3-A*: forward 5′-ACTGTGCTTACTGAACGGCCTC-3′ and reverse 5′-CCGGTCCTTGATCTTTCGGTTG-3′; *LMO3-B*: forward 5′-TGCAACTCAGACACGCCTAAG-3′ and reverse 5′-CCGGTCCTTGATCTTTCGGTTG-3′; *LMO1*: forward 5′-GCTCCACCCTCTACACCAAG-3′ and reverse 5′-CTGCCCTTCCTCATAGTCCA-3′; *LMO2*: forward 5′-AATGCGGGTGAAAGACAAAG-3′ and reverse 5′-CCCCAAAGTGCCTAAGAGTG-3′; *LMO4*: forward 5′-GCAAGGCAATGTGTATCATCT-3′ and reverse 5′-GCATTCTGCATTACTCTGACC-3′; *Ldb1*: forward 5′-CCAGGGAGCAGAAGACAGAA-3′ and reverse 5′-AGAGGCCCAGGTTCCAAG-3′; *Ldb2*: forward 5′-TAGCCCAAGTGCTGAAACAA-3′ and reverse 5′-TAAACTGCCCACAAAACCAA-3′; *TAL1*: forward 5′-GTTCTTAGGCTGCTGGGATG-3′ and reverse 5′-GATTTGGGACTGAGGGAAGA-3′; *HEN1*: forward 5′-AGAGACTGAGTCGGGCTTCA-3′ and reverse 5′-CAGGCGCAGAATCTCAATCT-3′; *HEN2*: forward 5′-CCCCAAGGGTTGTGGTTTTA-3′ and reverse 5′-TCTGAACTTCTGCCCTCATTCTTT-3′; and *GAPDH*: forward 5′-ACCTGACCTGCCGTCTAGAA-3′ and reverse 5′-TCCACCACCCTGTTGCTGTA-3′. Amplified products were electrophoretically separated on agarose gels and visualized by ethidium bromide staining. The gels were photographed under UV illumination.

Northern analysis. A human MTN blot (Clontech, Palo Alto, CA), a nylon membrane on which poly(A)$^+$ RNAs extracted from various human normal tissues were blotted, was used for analysis of the distribution of *LMO3* expression in human normal tissues. ^{32}P-labeled probe was prepared by random priming of the 2.5-kb restriction fragment of *LMO3* cDNA. The membrane was hybridized overnight at 65C in a solution containing 7.5% dextran sulfate, 1 mol/L NaCl, 1% *N*-lauroyl sarcosine, 100 μg/mL heat-denatured salmon sperm DNA, and the radiolabeled probe. The membrane was washed twice in 0.5 × SSC/0.1% *N*-lauroyl sarcosine at 50°C. Specific signals were obtained by autoradiography.

Section *in situ* hybridization. Section *in situ* hybridization was done as described previously (29). A riboprobe was synthesized with digoxygenin-UTP and T3 or T7 polymerase (Roche Molecular Biochemicals). The alkaline phosphatase reaction was done with nitroblue tetrazolium/5-bromo-4-chloro-3-indolyl phosphate (Roche Molecular Biochemicals). The riboprobe used for the section *in situ* hybridization were transcripts of the human cDNA fragments of the *LMO3* gene.

Immunohistochemistry. Neuroblastoma tissues were stained with immunoperoxidase method using anti-HEN2 antibody. They included unfavorable neuroblastomas with *MYCN* gene amplification and favorable neuroblastomas with a single copy of *MYCN* gene. Neuroblastoma specimens were fixed in 10% buffered formalin and embedded in paraffin, and 3 μm sections were applied to the immunostaining. Before incubation with anti-HEN2 antibody, the sections were treated with 0.05% Pronase in 0.05 mol/L Tris-HCl (pH 7.6) for 5 minutes. The sections were incubated with anti-HEN2 antibody, which was diluted to 1:200 at 4°C overnight. The biotin-streptavidin method (Nichirei, Tokyo, Japan) was done, and the sections were visualized with diaminobenzidine solution. The nuclei were counterstained with hematoxylin.

Immunofluorescent staining. COS7 cells were doubly transfected with the expression plasmids for HA-LMO3-A and FLAG-HEN2. Forty-eight hours after transfection, cells were fixed for 30 minutes with 3.7% formaldehyde in PBS and permeabilized with 0.2% Triton X-100 for 5 minutes, and nonspecific epitopes were blocked for 1 hour in PBS containing 3% bovine serum albumin. The cells were then incubated with a polyclonal anti-HA antibody (1:200 dilution, Medical and Biological Laboratories, Nagoya,

Japan) and a monoclonal anti-FLAG antibody (1:50, M2, Sigma Chemical). After three washes with PBS, cells were stained with a FITC- or a rhodamine-conjugated secondary antibody (1:200, Invitrogen). The coverslips were mounted onto glass slides, and the stained cells were viewed using a confocal laser scanning microscope (Olympus, Tokyo, Japan).

Western blot analysis and immunoprecipitation. After transfection, cells were rinsed twice with ice-cold PBS and then lysed immediately with SDS sample buffer. Equal amounts of proteins were separated under denaturing conditions by electrophoresis in 15% polyacrylamide gel containing SDS-PAGE and electrotransferred to polyvinylidene difluoride membrane (Immobilon-P, Millipore, Bedford, MA). After blocking in a solution containing 5% skim milk, the membrane was incubated with a monoclonal anti-FLAG, a polyclonal anti-HA, a polyclonal anti-LMO3, or a polyclonal anti-actin antibody (20-33, Sigma Chemical) and then incubated with a horseradish peroxidase–conjugated goat anti-mouse or anti-rabbit secondary antibody (Jackson ImmunoResearch Laboratories, West Grove, PA). Protein bands were visualized with an enhanced chemiluminescence (Amersham Pharmacia Biotech, Piscataway, NJ). For immunoprecipitation, transfected cells were lysed in EBC buffer [50 mmol/L Tris-HCl (pH 7.5), 120 mmol/L NaCl, 0.5% NP40, 1 mmol/L phenylmethylsulfonyl fluoride] containing protease inhibitor mixture (Sigma Chemical). The precleared soluble supernatants were mixed with a polyclonal anti-HA or a monoclonal anti-FLAG antibody and incubated for 2 hours at 4°C. Protein A-Sepharose beads were then added to the reaction mixtures and incubated for 1 hour at 4°C. The immune complexes were washed with the lysis buffer thrice at 4°C. The bound proteins were resuspended in SDS sample buffer, resolved by SDS-PAGE, and analyzed by Western blotting.

Cell proliferation and soft agar assay. Cells were seeded in triplicate in 24-well plates (5×10^3 per well) in culture medium containing 10% or 1% FBS. Cells were allowed to adhere to the bottom of the cell culture dish for 24 hours. At the indicated times, cells were trypsinized and cell counting was carried out using a Coulter Counter (Coulter Electronics Ltd., Hialeah, Finland). For soft agar assay, 2.5×10^3 cells of the stable transfectants or the parental SH-SY5Y cells were seeded in triplicate in 35-mm cell culture plates containing 0.2% agar and RPMI 1640 supplemented with 10% FBS. After 21 days, colonies with diameters >300 μm were scored as positive.

Tumor formation in nude mice. For tumor formation, 6-week-old female athymic *nu/nu* mice (Charles River Laboratory, Sulzfeld, Germany) were injected into the femur with 5×10^6 parental SH-SY5Y cells or SH-SY5Y cells transfected with the empty plasmid or with the expression plasmid encoding LMO3-A suspended in 100 μL PBS. Tumor size and body weight were measured once weekly and mice were sacrificed 7 weeks after injection. For histologic examinations, tumor tissues were fixed in fresh 10% buffered formalin and embedded in paraffin. The handling of animals was in accordance with the guidelines of the Chiba Cancer Center Research Institute (Chiba, Japan).

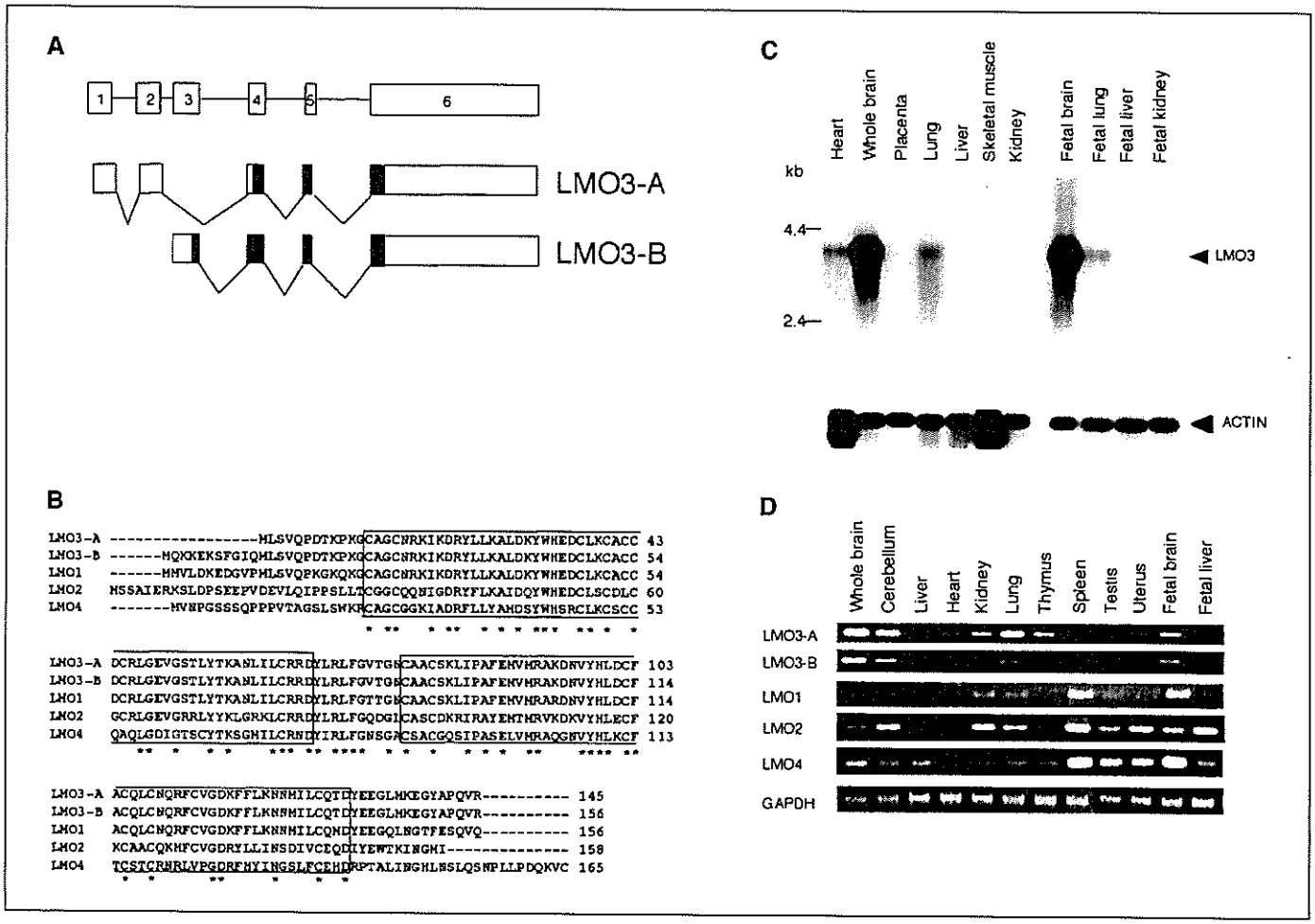

Figure 1. Identification of human LMO3-A and LMO3-B and their relation to the other LMO family members. *A*, schematic representation of the exons of human *LMO3* gene. *Solid* and *open boxes*, coding and untranslated regions, respectively. *B*, deduced amino acid sequences of human LMO3-A and LMO3-B and their alignments with those of human LMO1, LMO2, and LMO4. *Asterisks*, identical amino acid residues. Two LIM domains are *boxed*. *C*, tissue-specific expression of *LMO3*. Human multiple tissue Northern blots containing poly(A)$^+$ RNA were hybridized with a radiolabeled human *LMO3* cDNA (*top*) or with a radioactive probe derived from human *β-actin* cDNA (*bottom*). β-actin was used as a control for equal loading. The 2-kb band was hybridized ubiquitously, and an additional 1.8-kb band was hybridized in heart and skeletal muscle with the β-actin probe. *D*, coordinated expression of *LMO3-A* and *LMO3-B* in various human tissues. Total RNA isolated from the indicated human tissues was subjected to RT-PCR analysis to examine the expression levels of *LMO3-A*, *LMO3-B*, *LMO1*, *LMO2*, and *LMO4*. *GAPDH* expression is shown as an internal control.

Quantitative real-time PCR. Total RNA prepared from primary neuroblastomas was reverse transcribed into cDNA (SuperScript II kit) and subjected to the real-time PCR. The expression level of *GAPDH* was measured in all samples to normalize *LMO3* and *HEN2* expression according to the manufacturer's instructions (Applied Biosystems, Foster City, CA). Oligonucleotide primers and TaqMan probes, which were labeled at the 5′ end with the reporter dye 6-carboxyfluorescein (FAM) and at the 3′ end with the quencher dye 6-carboxytetramethylrhodamine (TAMRA), were as follows: *LMO3*: forward 5′-TCTGAGGCTCTT-TGGTGTAACG-3′, reverse 5′-CCAGGTGGTAAACATTGTCCTTG-3′, and probe 5′-FAM-AAACTGCGCTGCCTGTAGTAAGCTCATCC-TAMRA-3′ and *HEN2*: forward 5′-CCCCAAGGGTTGTGGTTTTA-3′, reverse 5′-TCTGAACTTCTGCCCTCATTCTTT-3′, and probe 5′-FAM-TTGAGTTCTCC-TACATTCATCCGCCACAA-TAMRA-3′. Amplification and detection were done using the ABI Prism 7700 Sequence Detection System (Applied Biosystems).

Statistical analysis. Student's *t* tests were used to explore possible associations between *LMO3* expression and other factors. Because the values of the *LMO3* expression were skewed, a log transformation was used to achieve the normality in the analyses using *t* test and Cox regression. The distinction between high and low levels of *LMO3* expression was based on the median value (low, *LMO3* < 0.2493 e.u.; high, *LMO3* > 0.2493 e.u.) regardless of tumor stage, *MYCN* copy number, or survival. The distinction between high and low levels of *HEN2* expression was based on the distribution of the values (low, undetectable; high, detectable). χ^2 tests were used to examine possible associations between *HEN2* expression and other factors, such as tumor stage. Kaplan-Meier survival curves were calculated, and survival distributions were compared using the log-rank test. Cox regression models were used to explore associations among *LMO3* expression, *HEN2* expression, age, *MYCN* amplification, mass screening, origin, and survival. Statistical significance was declared if $P < 0.05$. The statistical analysis was done using Stata Statistical Software Release 7.0 (Stata Corp., College Station, TX, 2001).

Results

Identification of the human *LMO3* gene. To identify the genes specifically involved in the genesis and progression of neuroblastoma, we have previously constructed cDNA libraries from the primary neuroblastomas and screened for the differentially expressed genes between the tumors with good and poor clinical outcome (25). One of the cDNA clones, *Nbla3267*, significantly overexpressed in the poor prognostic neuroblastomas contained a partial nucleotide sequence encoding a LMO family protein, LMO3. To obtain the missing 5′ part of the *LMO3* cDNA, we screened a cDNA library derived from human fetal brain. From ~6 × 10^5 recombinant phage clones, 10 independent phage clones were isolated. Sequence analysis

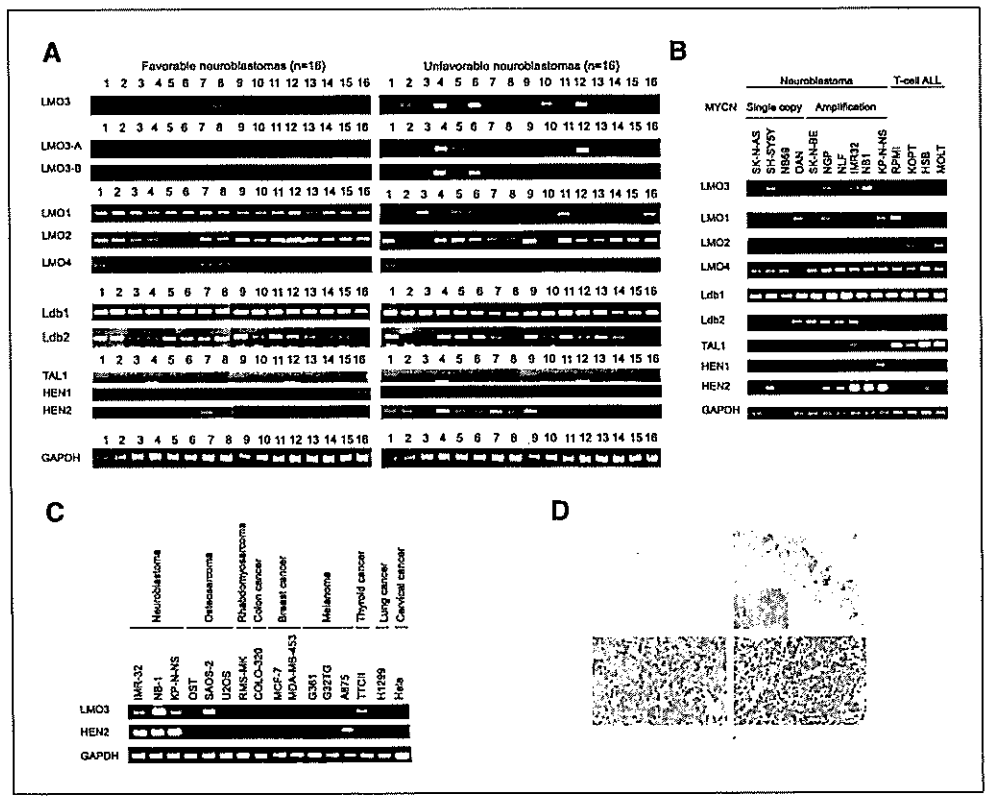

Figure 2. Increased expression of *LMO3* and *HEN2* in unfavorable neuroblastomas and neuroblastoma-derived cell lines. *A*, expression of *LMO3* and *LMO*-related genes in primary neuroblastomas with favorable (stage I, a single copy of *MYCN* and high expression of *TrkA*) and unfavorable (stages III and IV, *MYCN* amplification and decreased expression of *TrkA*) characteristics. Total RNA was isolated from the indicated neuroblastoma tissues, reverse transcribed, and amplified by PCR to examine the expression levels of *LMO3*, *LMO3-A*, *LMO3-B*, *LMO1*, *LMO2*, *LMO4*, *Ldb1*, *Ldb2*, *TAL1*, *HEN1*, and *HEN2*. Expression of *GAPDH* serves as an internal control. PCR products were visualized by ethidium bromide staining. *B*, expression of *LMO3* and *LMO*-related genes in neuroblastoma cell lines without *MYCN* amplification (SK-N-AS, SH-SY5Y, NB69, and OAN), neuroblastoma cell lines with *MYCN* amplification (SK-N-BE, NGP, NLF, IMR32, NB1, and KP-N-NS), and ALL cell lines (RPMI, KOPT, HSB, and MOLT). Total RNA prepared from the indicated cultured cells was subjected to RT-PCR analysis. Expression of *GAPDH* serves as an internal control. *C*, expression of *LMO3* and *HEN2* in various tumor-derived cell lines. Total RNA prepared from the indicated culture cells was subjected to RT-PCR analysis as described above. *D*, section *in situ* hybridization of neuroblastoma with the *LMO3* probe. Serial sections of the favorable neuroblastoma tissue (*top left* and *inset*) or the unfavorable one with *MYCN* amplification (*top right* and *inset*) were prepared, and expression of the *LMO3* gene was examined by section *in situ* hybridization. The *LMO3* transcripts are positive in unfavorable neuroblastoma. Immunohistochemical staining of HEN2 in primary neuroblastoma tissues. HEN2 is strongly positive in the nucleus of most tumor cells with *MYCN* amplification (*bottom right*), whereas it is negative in the favorable neuroblastoma tissue (*bottom left*).

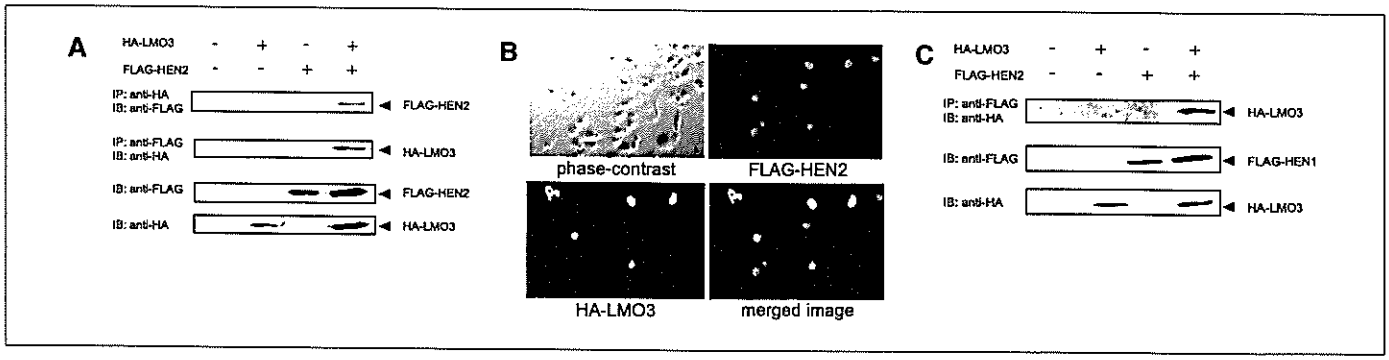

Figure 3. LMO3 interacts with HEN2 in mammalian cells. *A*, coimmunoprecipitation analysis. COS7 cells were transfected with the indicated expression plasmids. Forty-eight hours after transfection, whole cell lysates were prepared and subjected to the immunoprecipitation/Western analysis (*top* and *top middle*). Whole cell lysates were monitored on immunoblot for the expression of FLAG-HEN2 (*bottom middle*) and HA-LMO3-A (*bottom*). *B*, nuclear colocalization of LMO3 and HEN2 in cultured cells. COS7 cells were cotransfected with the expression plasmids for HA-LMO3-A and FLAG-HEN2. Forty-eight hours after transfection, cells were fixed and incubated with the polyclonal anti-HA and monoclonal anti-FLAG antibodies. Cells were then processed for double immunofluorescence using the FITC-conjugated anti-rabbit IgG (*green*) and with the rhodamine-conjugated anti-mouse IgG (*red*). The merged images (*yellow*) suggest the nuclear colocalization of LMO3 and HEN2. The phase-contrast images are also shown. *C*, coimmunoprecipitation of FLAG-HEN1 and HA-LMO3. Whole cell lysates prepared from COS7 cells transfected with the indicated combinations of the expression plasmids were immunoprecipitated with the anti-FLAG antibody followed by immunoblotting with the anti-HA antibody (*top*). Levels of FLAG-HEN1 and HA-LMO3 were also examined by immunoblotting with the anti-FLAG antibody (*middle*) and with the anti-HA antibody (*bottom*), respectively.

revealed that they were divided into two types, designated LMO3-A (145 amino acids) and LMO3-B (156 amino acids), with the different translation initiation sites. The NH_2-terminal region of LMO3-A was identical to that of the previously reported LMO3 protein (11). As shown in Fig. 1*A*, the putative translation initiation sites of LMO3-A and LMO3-B were located within exons 4 and 3, respectively. Because *LMO3* is a single gene, it is likely that LMO3-A and LMO3-B arise from differential splicing

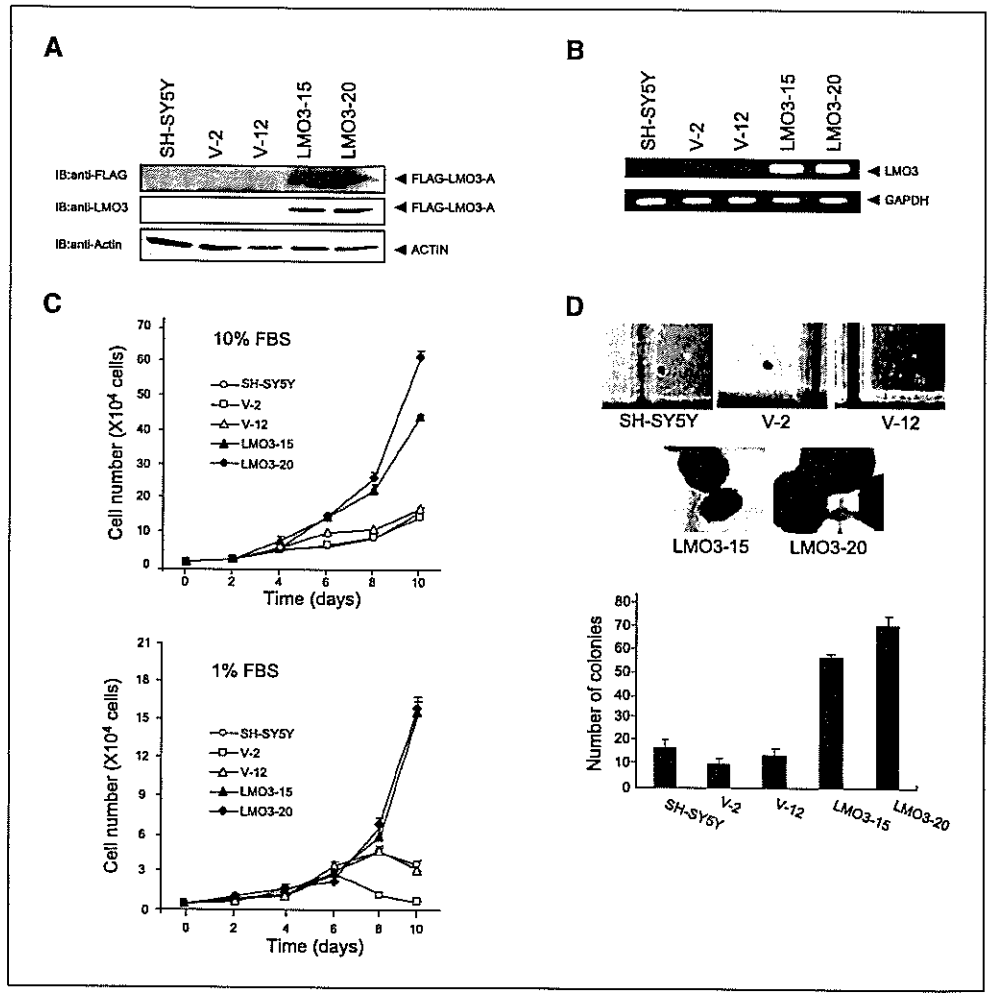

Figure 4. Growth-promoting activity of LMO3 in SH-SY5Y cells. *A*, stable SH-SY5Y transfectants expressing exogenous FLAG-LMO3-A. SH-SY5Y cells were stably transfected with the empty plasmid or with the expression plasmid for FLAG-LMO3-A and maintained in the presence of G418 (at a final concentration of 400 μg/mL) for 3 weeks. Whole cell lysates prepared from the indicated drug-resistant cell clones in addition to the parental SH-SY5Y cells were subjected to Western blot analysis using the anti-FLAG (*top*), anti-LMO3 (*middle*), or anti-actin (*bottom*) antibody. *B*, RT-PCR analysis of LMO3 in the indicated stable transfectants along with the parental SH-SY5Y cells. Expression of GAPDH serves as an internal control. *C*, effects of LMO3 overexpression on cell growth in SH-SY5Y cells. SH-SY5Y cells and the indicated transfectants were grown in the culture medium containing 10% (*top*) or 1% (*bottom*) FBS. Cells were harvested at 48-hour time intervals and number of cells was counted in triplicate. *Points*, means from three independent experiments; *bars*, SE. *D*, anchorage-independent growth of LMO3-overexpressing transfectants. The parental SH-SY5Y cells and the indicated transfectants (2.5 × 10^3 cells per dish) were grown in soft agar medium. After 3 weeks of culture, cells were examined by phase-contrast microscopy (*top*), and the numbers of colonies with a diameter of >300 μm were counted (*bottom*). *Columns*, means from three independent experiments; *bars*, SE.

or alternative promoter usage. Amino acid sequence alignment of LMO3 with the other LMO family proteins (LMO1, LMO2, and LMO4) showed a significant homology among them (Fig. 1*B*). LIM domains of LMO3 presented 98%, 60%, and 55% amino acid homology with those of LMO1, LMO2, and LMO4, respectively.

To determine the expression pattern of human *LMO3* mRNA, we did Northern blot analysis on a human multiple tissues blot using -actin as a control. As shown in Fig. 1*C*, *LMO3* mRNA (~4 kb) was abundantly expressed in brain and at relatively low levels in the heart and lung but not in the other tissues examined. Similar to the adult tissues, *LMO3* mRNA was expressed predominantly in fetal brain, with a lower level in fetal lung. We then compared the tissue distribution of *LMO3-A* expression with those of *LMO3-B* and the other *LMO* family gene expression in various human adult and fetal tissues by RT-PCR (Fig. 1*D*). The expression pattern of *LMO3-A* was similar to that of *LMO3-B*, with relatively higher levels in brain, cerebellum, and fetal brain. In contrast, *LMO2* and *LMO4* were expressed ubiquitously in human tissues, and *LMO1* was expressed at higher levels in spleen and fetal brain.

Expression of *LMO3* and *HEN2* in aggressive neuroblastomas. As described previously, LMO family protein interacts with the nuclear LIM domain–binding protein 1 and 2 (Ldb1 and Ldb2), which act as adaptors for several LIM domain–containing proteins (30–32), and also binds to the basic helix-loop-helix transcription factor, TAL1, to regulate its transcriptional activity (12, 33, 34). Of interest, HEN1 and HEN2 were previously identified based on their homology with TAL1, and it was shown that LMO3 was associated with HEN1 (35). Furthermore, TAL1 was coexpressed with LMO1 or LMO2 in T-cell ALL (36), and double transgenic mice overexpressing TAL1 and LMO1 or LMO2 developed leukemia (37). As shown in Fig. 2*A*, *LMO3* (A and B) and *HEN2* were expressed at higher levels in unfavorable neuroblastomas compared with favorable tumors, whereas the levels of *LMO1* expression were predominantly high in the favorable tumors. No significant changes in the expression levels of *LMO2*, *Ldb1*, and *Ldb2* were detected between unfavorable and favorable neuroblastomas. *LMO4*, *TAL1*, and *HEN1* showed extremely low levels of expression in both types of neuroblastoma. We then studied the expression of these genes in 10 neuroblastoma and 4 T-cell ALL cell lines to examine the presence or absence of the lineage specificity, neuronal or hematopoietic. Consistent with the previous reports (36), *LMO2* and *TAL1* were coexpressed in T-cell ALL-derived cell lines (RPMI, KOPT, HSB, and MOLT; Fig. 2*B*). However, of interest, *LMO3* and *Ldb2* were expressed predominantly in neuroblastoma cell lines compared with the leukemia-derived lines. In addition, *HEN2* tended to be less highly expressed in leukemia cells compared with neuroblastoma cells. *HEN1* expression was also restricted to neuroblastoma but limited to only a few cell lines. On the other hand, there was no difference in the expression of *LMO4* and *Ldb1* between neuroblastoma-derived and T-cell ALL-derived cell lines. Interestingly, coexpression of *LMO3* and *HEN2* was observed in the majority of neuroblastoma cell lines but not in the other tumor-derived cell lines with different origin (Fig. 2*C*). These results revealed that only *LMO3* and *HEN2* were expressed at high levels in aggressive neuroblastomas in a neuronal-specific pattern.

Figure 2*D* shows the results of *in situ* hybridization for *LMO3* in primary neuroblastomas. *LMO3* mRNA was expressed in a stage IV neuroblastoma with *MYCN* amplification, whereas it was negative in a stage I tumor with a single copy of *MYCN* and high expression of *TrkA*. Unfortunately, our antibody raised against human LMO3 protein did not work for the immunohistochemical analysis. The immunostaining of HEN2 was also strongly positive in the nuclei of most tumor cells in *MYCN*-amplified neuroblastoma, albeit it was negative in favorable subset of the tumor (Fig. 2*D*).

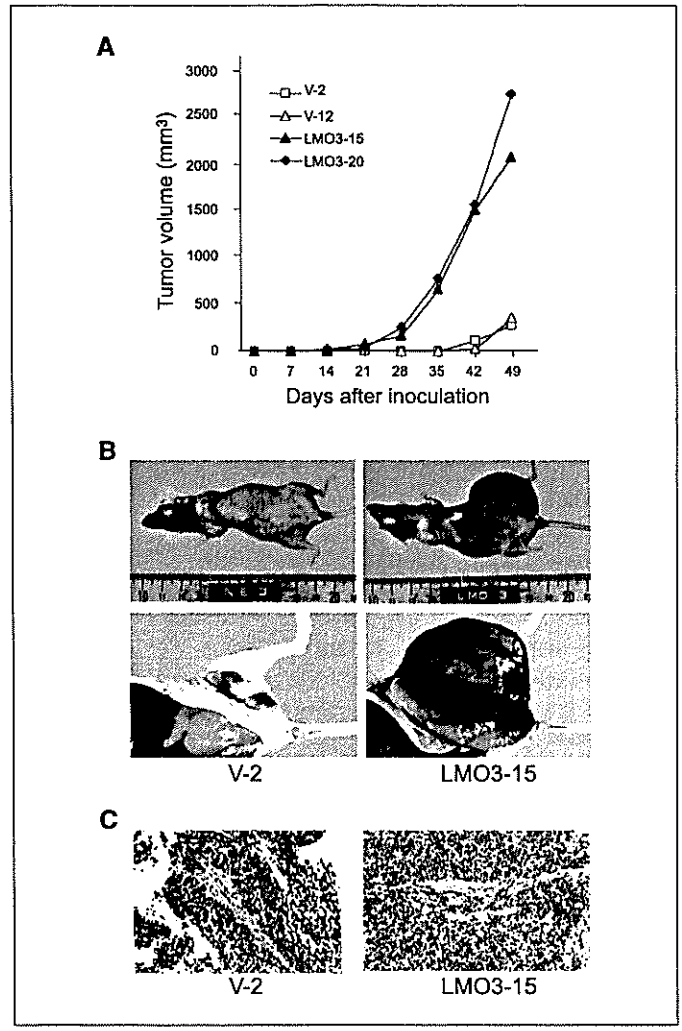

Figure 5. Tumor growth in nude mice. *A*, nude mice were injected s.c. with 5×10^6 of SH-SY5Y cells or the indicated stable transfectants and tumor volumes were estimated weekly. *Points*, mean of 8 to 11 independent tumors. *B*, photographs of the tumors 49 days after s.c. injection of V-2 (*left*) and LMO3-15 cells (*right*) into nude mice. *C*, paraffin sections of the tumors arising from V-2 (*left*) and LMO3-15 cells (*right*) were stained with H&E.

LMO3 physically interacts with HEN2. Because LMO3 and HEN2 were coexpressed in the majority of unfavorable neuroblastomas as well as neuroblastoma cell lines, we examined whether LMO3 could interact with HEN2 in mammalian cells. Whole cell lysates prepared from COS7 cells transfected with the expression plasmids for HA-tagged LMO3 and FLAG-tagged HEN2 were immunoprecipitated with the anti-HA or with the anti-FLAG antibody followed by immunoblotting with the anti-FLAG or with the anti-HA antibody, respectively. As shown in Fig. 3*A*, FLAG-HEN2 was coimmunoprecipitated with HA-LMO3. We then examined the subcellular distribution of LMO3 and

HEN2. COS7 cells were cotransfected with the expression plasmids for HA-LMO3 and FLAG-HEN2 and double stained with anti-HA and anti-FLAG antibodies. As shown in Fig. 3*B*, LMO3 as well as HEN2 appear exclusively nuclear. On closer inspection by merging two images, these two proteins colocalized in the nucleus. Consistent with the previous reports (35), HA-LMO3 was coimmunoprecipitated with FLAG-HEN1 under our experimental conditions (Fig. 3*C*).

Overexpression of LMO3 accelerates growth of SH-SY5Y neuroblastoma cells. We addressed the question whether LMO3 could induce cell growth of neuroblastoma. To this end, we transfected the expression plasmid for FLAG-LMO3-A or the empty plasmid into SH-SY5Y neuroblastoma cells and established two stable transfectants overexpressing FLAG-LMO3-A (named as LMO3-15 and LMO3-20). As shown in Fig. 4*A*, the expression levels of FLAG-LMO3-A were higher in LMO3-15 and LMO3-20 cells than in the parental SH-SY5Y and the control transfectants (V-2 and V-12). LMO3-15 expressed FLAG-LMO3-A at the level comparable with that in LMO3-20. Similar results were also obtained by RT-PCR analysis (Fig. 4*B*). No obvious morphologic changes could be observed in LMO3-15 and LMO3-20 cells (data not shown). As shown in Fig. 4*C*, LMO3-15 and LMO3-20 cells proliferated at a much faster rate than the control transfectants and SH-SY5Y cells in culture medium containing 10% serum. More importantly, LMO3-15 and LMO3-20 cells continued to grow exponentially even in the low serum culture medium, whereas the growth of the vector-transfected cells as well as SH-SY5Y cells was significantly suppressed under this condition.

To examine whether the LMO3-A-overexpressing cells have an ability to grow in soft agar medium, each transfectants were cultured in soft agar medium for 3 weeks. The numbers of colonies with diameters >300 μm formed by each transfectants in soft agar were scored. LMO3-15 and LMO3-20 cells formed large distinct colonies and showed a statistically significant increase in the number of colonies compared with the vector-transfected cells and SH-SY5Y cells (Fig. 4*D*). These results strongly suggest that overexpression of LMO3 is sufficient to induce malignant transformation in neuroblastoma cells. We also tried to obtain the cells stably transfected with HEN2 but never been successful with unknown reason.

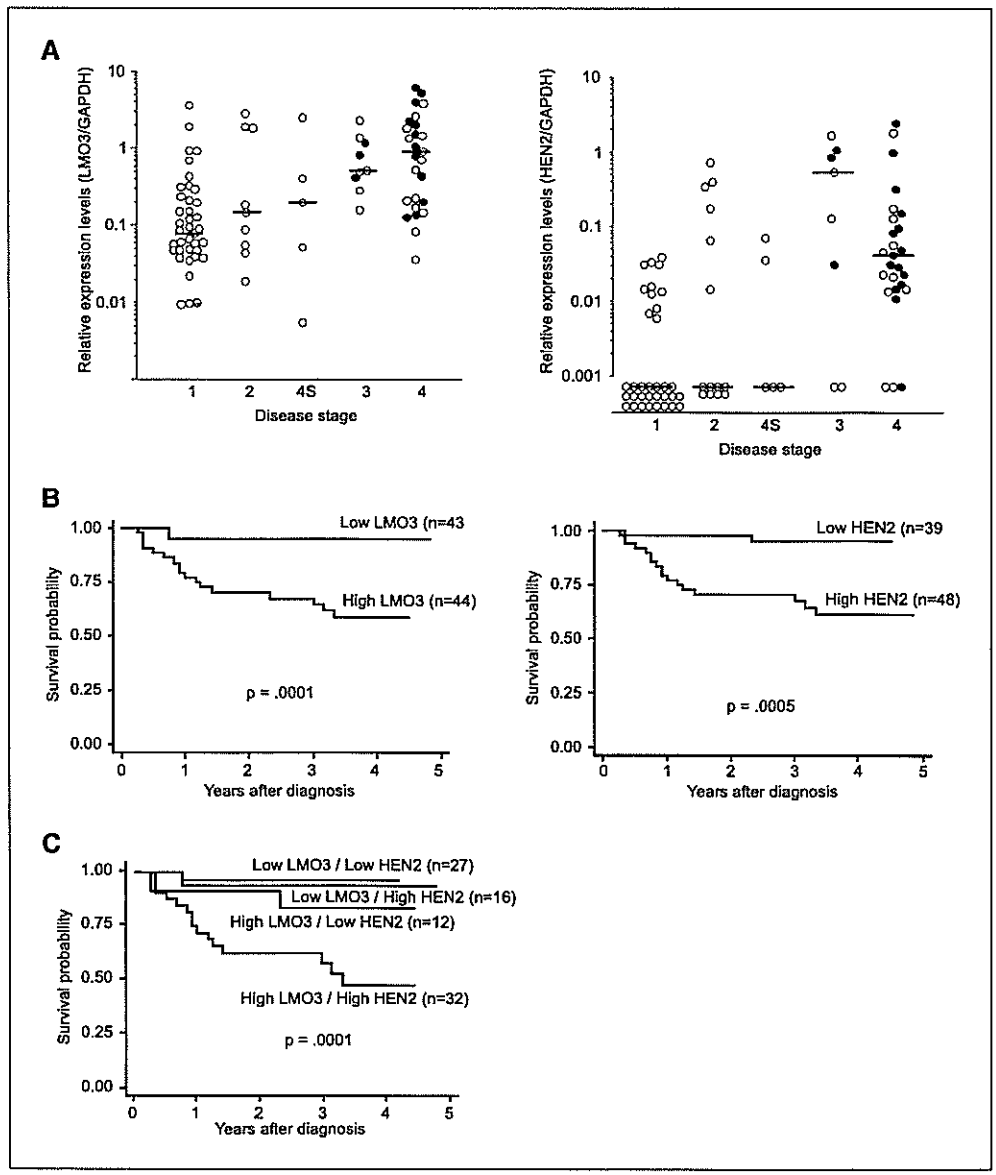

Figure 6. Expression of *LMO3* and *HEN2* mRNA in 87 primary neuroblastomas. *A*, expression levels of *LMO3* (*left*) and *HEN2* (*right*) transcripts in 87 primary neuroblastoma samples categorized by the patient's clinical stage were examined by a quantitative real-time RT-PCR. Relative expression levels of *LMO3* or *HEN2* mRNA were determined by calculating the ratio between *GAPDH* and *LMO3* or *HEN2*. *Bars*, median levels of *LMO3* or *HEN2* expression in each stage; *open* and *closed circles*, samples from patients who are alive and dead, respectively. *B* and *C*, Kaplan-Meier survival curves of patients with neuroblastomas based on high or low expression of *LMO3*, *HEN2* (*B*), or *LMO3* and *HEN2* (*C*).

LMO3 induces marked tumor growth in nude mice. SH-SY5Y cells with a single copy of *MYCN* form tumors in nude mice, although the growth rate is slow compared with that of the other neuroblastoma cell lines with *MYCN* amplification (38). To examine whether overexpression of LMO3 in SH-SY5Y cells could affect the tumor growth *in vivo*, we injected the each transfectants into the left flank of athymic nude mice, and the tumor volumes were measured weekly. V-2 and V-12 cells slowly formed tumors with similar kinetics and of similar sizes 35 to 42 days after injection (Fig. 5*A*). In contrast, the tumors grew rapidly in nude mice implanted with LMO3-15 or LMO3-20 cells. The sizes of the excised tumors from the LMO3-15-implanted mice on day 49 were >10-fold larger than those of control mice (Fig. 5*B*) and showed histologically undifferentiated neuroblastoma with small round cell shapes and small amounts of stromal components (Fig. 5*C*).

Expression of *LMO3* and *HEN2* is associated with a poor outcome of neuroblastoma. To verify whether a significant relationship could be observed between the expression of *LMO3* and/or *HEN2* in primary neuroblastomas and the patients' survival, we quantitatively measured the expression levels of *LMO3* and *HEN2* mRNA in 87 primary tumors by using a quantitative real-time RT-PCR. The values of the levels of *LMO3* and *HEN2* expression were normalized to that of *GAPDH* expression [relative expression values (REV)]. The high level of *LMO3* expression was significantly associated with high expression of *HEN2* (Student's *t* tests, mean ± SE: 1.43 ± 0.27 REV, n = 48 versus 0.54 ± 0.17 REV, n = 39; P = 0.001), older age (≥1-year-old: 1.37 ± 0.29, n = 32 versus <1-year-old: 0.84 ± 0.21, n = 55; P = 0.008), advanced disease stages (stages III + IV: 1.83 ± 0.35, n = 34 versus stages I + II + IVS: 0.52 ± 0.14; P < 0.00005; Fig. 6*A*), low levels of *TrkA* expression (low TrkA: 1.63 ± 0.34, n = 37 versus high *TrkA*: 0.59 ± 0.15, n = 50; P = 0.0003), *MYCN* amplification (amplification: 1.91 ± 0.44, n = 27 versus single copy: 0.64 ± 0.13, n = 60; P = 0.0002), and sporadic cases of neuroblastoma (sporadic: 1.68 ± 0.32, n = 39 versus mass screening: 0.51 ± 0.14, n = 48; P < 0.00005). The high level of *HEN2* expression was also significantly correlated with high expression of *LMO3* (χ^2 tests: P = 0.001), older age (P < 0.0005), advanced stages (P < 0.0005; Fig. 6*B*), low *TrkA* expression (P < 0.0005), *MYCN* amplification (P < 0.0005), and sporadic cases of neuroblastoma (P < 0.0005). Thus, high expression of *LMO3* and *HEN2* was well associated with conventional markers indicating the poor prognosis of neuroblastoma.

We next tested if expression levels of *LMO3* and *HEN2* could have prognostic significance in primary neuroblastomas. The results for log-rank tests showed that high expression of *LMO3* or *HEN2* was significantly associated with poor survival (P = 0.0002 and 0.0005, respectively; Fig. 6*C* and *D*). Remarkably, the combination of high expression of both *LMO3* and *HEN2* showed the significantly worse prognosis compared with the other combinations of *LMO3* and *HEN2* expression levels as shown in Fig. 6*E*. As expected, older patients and the patients with advanced tumors, low expression of *TrkA*, amplified *MYCN*, and the tumors found by mass screening were associated with short time to survival (P < 0.00005). However, the adrenal origin of the tumor was not associated with the outcome (P = 0.19; data not shown).

The univariate analysis suggested that *LMO3* expression (P < 0.0005), *HEN2* expression (P = 0.004), age (P < 0.0005), *MYCN* amplification (P < 0.0005), and mass screening (P = 0.001) were of prognostic importance, supporting the results of the log-rank test (Table 1). Furthermore, the multivariate analysis showed that

Table 1. Simple Cox regression models using LMO3 expression and dichotomous factors of HEN2 expression, age, MYCN amplification, mass screening, and origin (n = 87)

Model	Factor	P	Hazard ratio (95% confidence interval)
A	LMO3 expression (high vs low)	<0.0005	1.80 (1.32-2.47)
B	HEN2 expression (high vs low)	0.004	8.69 (2.00-37.7)
C	Age (≥1 vs <1 y)	<0.0005	8.75 (2.87-26.7)
D	MYCN amplification (1 copy vs >1 copy)	<0.0005	0.049 (0.014-0.171)
E	Mass screening (+ vs −)	0.001	0.032 (0.004-0.237)
F	Origin (adrenal gland vs others)	0.20	2.06 (0.684-6.23)

NOTE: All variables with two categories, except *LMO3* expression (log). Hazard ratio shows the relative risk of death of first category relative to the second. Because all patients with advanced tumor stages and low expression of *TrkA* had died of the tumor, a Cox regression model with the tumor stage or *TrkA* expression was not fitted.

Table 2. Multiple Cox regression models using LMO3 expression and dichotomous factors of HEN2 expression, age, MYCN amplification, mass screening, and origin (n = 87)

Model	Factor	P	Hazard ratio (95% confidence interval)
A	LMO3 expression (high vs low)	0.005	1.61 (1.16-2.23)
	HEN2 expression (high vs low)	0.029	5.32 (1.19-23.9)
B	LMO3 expression (high vs low)	0.005	1.62 (1.15-2.28)
	Age (>1 vs <1 y)	0.002	5.79 (1.86-18.1)
C	LMO3 expression (high vs low)	0.066	1.36 (0.98-1.89)
	MYCN amplification (1 copy vs >1 copy)	<0.0005	0.075 (.02-.282)
D	LMO3 expression (high vs low)	0.044	1.42 (1.01-2.01)
	Mass screening (+ vs −)	0.005	0.051 (0.007-0.404)
E	LMO3 expression (high vs low)	<0.0005	1.78 (1.31-2.41)
	Origin (adrenal gland vs others)	0.21	2.02 (0.666-6.12)

NOTE: All variables with two categories, except *LMO3* expression (log). Hazard ratio shows the relative risk of death of first category relative to the second.

LMO3 expression was significantly associated with survival after controlling *HEN2* expression ($P = 0.005$), age ($P = 0.005$), mass screening ($P = 0.044$), and origin ($P < 0.0005$), suggesting that *LMO3* expression was an independent prognostic factor from the other factors (Table 2). *LMO3* expression was marginally associated with survival after controlling *MYCN* amplification ($P = 0.066$). On the other hand, because *HEN2* expression was highly associated with age, *MYCN* amplification, and mass screening, it was not significantly associated with survival after controlling age, *MYCN* amplification, and mass screening in the corresponding multiple Cox regression models (data not shown).

Discussion

In the present study, we have identified that both *LMO3* and *HEN2* are expressed at higher levels in aggressive neuroblastomas especially with *MYCN* amplification than those with favorable prognosis. Coexpression of *LMO3* and *HEN2* has been observed almost exclusively in neuroblastoma cell lines, not the other lines, suggesting that their expression and function are neuronal specific. Furthermore, LMO3 physically interacted with HEN2 in mammalian cells. The functional significance of LMO3 expression was shown by a stable transfection into SH-SY5Y neuroblastoma cells, colony formation in soft agar, and tumor growth in nude mice, all of which have suggested that LMO3, probably by interacting with endogenous HEN2, markedly promotes the tumor growth. Indeed, the tumors with high expression of both *LMO3* and *HEN2* have shown the worst prognosis in the analysis of 87 primary neuroblastomas. Thus, our results suggested that, in concert with HEN2, the neuronal specifically expressed LMO3 plays an important role in the tumorigenesis of neuroblastoma. Our observation is strikingly intriguing because that *LMO1* or *LMO2* is already known to be the oncogene in T-cell acute lymphoblastic leukemia and that *LMO4* has recently been implicated in the genesis of breast cancer (4, 9).

We have identified a *Nbla3267/LMO3* clone from the screening of differentially expressed genes between favorable and unfavorable subsets of neuroblastoma. *LMO3* was one of the genes expressed at higher levels in the latter than the former (24), like *MYCN* oncogene and *DDX1*, a DEAD box gene coamplified with *MYCN* in aggressive neuroblastomas. In the development of hematopoietic system, LMO1 and LMO2 form a transcriptional complex with Ldb1, a LIM domain–binding protein, and a basic helix-loop-helix protein TAL1, which was identified as an oncogene at the translocation breakpoint in T-cell ALL (4–7). From the analogy with the LMO1 or LMO2 transcriptional machinery in T-cell ALL, we searched for the similar complex in the neuronal system by using the different subsets of primary neuroblastoma and the cell lines in comparison with the T-cell ALL cell lines. As a result, the neuronal-specific pattern of expression was observed in *LMO3*, *Ldb2*, *HEN1*, and *HEN2*, among which *LMO3* and *HEN2* were significantly highly expressed in the unfavorable subset of neuroblastomas with *MYCN* amplification compared with the favorable subset. This result strongly suggested that *LMO3* may function in collaboration with *HEN2* in advanced stages of neuroblastoma. Indeed, both genes were coexpressed only in neuroblastoma derived-cell lines, not in other tumor-derived ones, suggesting that their expression is lineage specific. Furthermore, LMO3 and HEN2 physically interacted in mammalian cells, albeit with weak interaction between LMO3 and HEN1 (35). Thus, these results also suggest that LMO3 and HEN2 form a neuronal cassette mimicking the hematopoietic complex composed of LMO2 and TAL1 and regulate the growth of neuroblastoma.

The neuronal-specific basic helix-loop-helix transcription factors, HEN1 and HEN2, were originally identified from the cDNA library of a neuroblastoma cell line based on cross-hybridization with TAL1 (14, 15). Their expression was restricted to the developing nervous system and a neuroblastoma cell line. However, their function has long been unclear. Recently, Bao et al. have reported that HEN1 interacts with LMO proteins by yeast two-hybrid screen and that *Xenopus* HEN1, in concert with XLMO3, is a critical regulator of neurogenesis (35). This prompted us to test our hypothesis both *in vitro* and *in vivo*. As the results, we found that the SH-SY5Y neuroblastoma cells stably overexpressing LMO3, presumably by acting with endogenous HEN2, gained rapid cell growth in the culture medium with 10% or 1% serum, in the soft agar medium, and in nude mice. These suggested that LMO3 is a neuronal-specific oncogene in neuroblastoma, without any rearrangement of the *LMO3* gene (data not shown). However, we failed to establish a stable SH-SY5Y cell line transfected with HEN2. It is presumed that overexpression of HEN2 might have caused cell death or growth arrest in the cells, albeit the reason is elusive.

The double transgenic mice overexpressing LMO2 and TAL1 displayed a more rapid development of leukemia compared with those overexpressing LMO2 alone, suggesting that LMO2 and TAL1 act synergistically through their complex formation in the development of leukemia (13). Of note, Ono et al. reported that LMO2 and TAL1 act as cofactors for GATA3 to induce the expression of the *retinaldehyde dehydrogenase 2* gene in T-cell ALL (39). On the other hand, a stable complex comprising LMO2, TAL1, and GATA1 was required to promote erythroid differentiation (32). Therefore, LMO3 and HEN2 may also form a nuclear complex, including family members of GATA to regulate cell growth and differentiation in neuroblastoma. Our preliminary data have suggested that GATA2, GATA3, GATA4, and GATA6 are highly expressed in neuroblastoma cell lines, among which GATA4 and GATA6 are predominantly coexpressed in neuroblastoma cell lines compared with T-cell ALL lines. Thus, LMO3 and HEN2, in collaboration with GATA and Ldb families, may play a role in determining cell fate in both neural development and neuroblastoma genesis, although this hypothesis needs to be elucidated. Recently, it has been shown that LMO3 enhanced the ability of HEN1 through the physical interaction to transactivate the expression of *Neurogenin-1* as well as *NeuroD* and thereby induced the neuronal differentiation in frog embryos (35). We tested if this is the case in the neuroblastoma cells. However, our preliminary results suggested that the LMO3/HEN2 complex does not transactivate the *Neurogenin-1* as well as *NeuroD* promoter in neuroblastoma cell lines,[5] although it is unclear if the complex could work in normal neuronal development. Thus, like LMO2, alterations in the LMO3-containing transcriptional complex might differentially regulate expression of the downstream target genes closely involved in neuronal differentiation or tumor formation.

[5] Unpublished data.

It is striking that high levels of expression of both *LMO3* and *HEN2* are significantly associated with the poor prognosis in primary neuroblastomas. This clearly reflects how importantly both genes are functioning in the progression of neuroblastoma *in vivo*. Of interest, expression of either gene is well correlated with *MYCN* amplification, raising the possibility that they might be the downstream targets of MYCN. However, we could not confirm it in human neuroblastoma cell line SH-EP in which MYCN was regulated under the control of the rTet-inducible expression system (40). In agreement with this, cDNA microarray-based screening for the genes induced in the *MYCN*-amplified neuroblastoma cells thus far failed to detect either LMO3 or HEN2 (41, 42). The link between LMO family molecules and the other oncogenes or tumor suppressor genes is also important. Despite the lack of prognostic significance, LMO4 overexpressed in breast cancer seems to be indispensable in the mammary carcinogenesis because it interacts with both BRCA1 and CtIP to repress the BRCA1 function (10). This suggests that, similarly to LMO4, LMO3 may also have the interacting partners related to the tumorigenesis. Thus, LMO3 and HEN2 as well as their associated molecules might be good candidates for the future targets of the therapy against aggressive neuroblastomas.

Acknowledgments

Received 12/28/2004; revised 3/9/2005; accepted 3/23/2005.

Grant support: Grant-in-Aid from the Ministry of Health, Labour and Welfare for Third Term Comprehensive Control Research for Cancer, Grant-in-Aid for Scientific Research on Priority Areas from the Ministry of Education, Culture, Sports, Science and Technology, Japan, and Grant-in-Aid for Scientific Research from Japan Society for the Promotion of Science. M. Aoyama is an awardee of the Research Resident Fellowship from the Foundation for Promotion of Cancer Research in Japan.

The costs of publication of this article were defrayed in part by the payment of page charges. This article must therefore be hereby marked *advertisement* in accordance with 18 U.S.C. Section 1734 solely to indicate this fact.

We thank S. Sakiyama for critical reading of the article; A. Morohashi, N. Kitabayashi, H. Murakami, and N. Sugimitsu for excellent technical assistance; and the following institutions and hospitals for supplying the tumor samples: Department of Pediatric Surgery, Iwaki Kyoritsu Hospital; Departments of Pediatrics and Pediatric Surgery, Aichi Medical University; Department of Pediatrics, Nara Hospital; Department of Pediatrics, Kyoto Prefectural University of Medicine; Department of Pediatric Surgery, Kimitsu Central Hospital; Department of Surgery, Gunma Children's Medical Center; Department of Pediatrics, Sapporo National Hospital; Departments of Pediatrics, Pediatric Surgery, and General Surgery, Jichi Medical School; Departments of Pediatrics and Pediatric Surgery, Kagoshima University; Department of Pediatrics, Juntendo University; Department of Pediatric Surgery, Showa University; Department of Pediatric Surgery, Niigata University; Departments of Surgery and Pathology, Chiba Children's Hospital; Department of Pediatric Surgery, Chiba University; Department of Pediatric Surgery, Osaka City General Hospital; Department of Pediatric Surgery, Tsukuba University; Department of Pediatric Surgery, Tokai University; Department of Surgery, Tokyo Metropolitan Kiyose Children's Hospital; Department of Pediatric Surgery, Tohoku University; Tumor Board, Hyogo Prefectural Kobe Children's Hospital; and First Department of Surgery, Hokkaido University.

References

1. Dawid IB, Breen JJ, Toyama R. LIM domains: multiple roles as adaptors and functional modifiers in protein interactions. Trends Genet 1998;14:156–62.
2. Sanchez-Garcia I, Rabbitts TH. The LIM domain: a new structural motif found in zinc-finger-like proteins. Trends Genet 1994;10:315–20.
3. Dawid IB, Toyama R, Taira M. LIM domain proteins. C R Acad Sci III 1995;318:295–306.
4. Rabbitts TH. LMO T-cell translocation oncogenes typify genes activated by chromosomal translocations that alter transcription and developmental processes. Genes Dev 1998;12:2651–7.
5. McGuire EA, Rintoul CE, Sclar GM, Korsmeyer SJ. Thymic overexpression of Ttg-1 in transgenic mice results in T-cell acute lymphoblastic leukemia/lymphoma. Mol Cell Biol 1992;12:4186–96.
6. Fisch P, Boehm T, Lavenir I, et al. T-cell acute lymphoblastic lymphoma induced in transgenic mice by the RBTN1 and RBTN2 LIM-domain genes. Oncogene 1992;7:2389–97.
7. Neale GA, Rehg JE, Goorha RM. Disruption of T-cell differentiation precedes T-cell tumor formation in LMO-2 (rhombotin-2) transgenic mice. Leukemia 1997;3:289–90.
8. Kenny DA, Jurata LW, Saga Y, Gill GN. Identification and characterization of LMO4, an LMO gene with a novel pattern of expression during embryogenesis. Proc Natl Acad Sci U S A 1998;95:11257–62.
9. Visvader JE, Venter D, Hahm K, et al. The LIM domain gene LMO4 inhibits differentiation of mammary epithelial cells *in vitro* and is overexpressed in breast cancer. Proc Natl Acad Sci U S A 2001;98:14452–7.
10. Sum EY, Peng B, Yu X, et al. The LIM domain protein LMO4 interacts with the cofactor CtIP and the tumor suppressor BRCA1 and inhibits BRCA1 activity. J Biol Chem 2002;277:7849–56.
11. Foroni L, Boehm T, White L, et al. The rhombotin gene family encode related LIM-domain proteins whose differing expression suggests multiple roles in mouse development. J Mol Biol 1992;226:747–61.
12. Wadman I, Li J, Bash RO, et al. Specific *in vivo* association between the bHLH and LIM proteins implicated in human T cell leukemia. EMBO J 1994; 13:4831–9.
13. Larson RC, Lavenir I, Larson TA, et al. Protein dimerization between Lmo2 (Rbtn2) and Tal1 alters thymocyte development and potentiates T cell tumorigenesis in transgenic mice. EMBO J 1996;15: 1021–7.
14. Brown L, Espinosa R III, Le Beau MM, Siciliano MJ, Baer R. HEN1 and HEN2: a subgroup of basic helix-loop-helix genes that are coexpressed in a human neuroblastoma. Proc Natl Acad Sci U S A 1992;89:8492–6.
15. Begley CG, Lipkowitz S, Gobel V, et al. Molecular characterization of NSCL, a gene encoding a helix-loop-helix protein expressed in the developing nervous system. Proc Natl Acad Sci U S A 1992;89:38–42.
16. Brodeur GM, Azar C, Brother M, et al. Effect of genetic factors on prognosis and treatment. Cancer 1992;70:1685–94.
17. Brodeur GM, Nakagawara A. Molecular basis of clinical heterogeneity in neuroblastoma. J Pediatr Hematol Oncol 1992;14:111–6.
18. Brodeur GM, Seeger RC, Schwab M, Varmus HE, Bishop JM. Amplification of N-*myc* in untreated human neuroblastomas correlates with advanced disease stage. Science 1984;224:1121–4.
19. Seeger RC, Brodeur GM, Sather H, et al. Association of multiple copies of the N-*myc* oncogene with rapid progression of neuroblastomas. N Engl J Med 1985;313: 1111–6.
20. Nakagawara A, Arima M, Azar CG, Scavarda NJ, Brodeur GM. Inverse relationship between trk expression and N-*myc* amplification in human neuroblastomas. Cancer Res 1992;52:1364–8.
21. Nakagawara A, Arima-Nakagawara M, Scavarda NJ, Azar CG, Cantor AB, Brodeur GM. Association between high levels of expression of the TRK gene and favorable outcome in human neuroblastoma. N Engl J Med 1993; 328:847–54.
22. Gross N, Beretta C, Peruisseau G, Jackson D, Simmons D, Beck D. CD44H expression by human neuroblastoma cells: relation to MYCN amplification and lineage differentiation. Cancer Res 1994;54: 4238–42.
23. Berwanger B, Hartmann O, Bergmann E, et al. Loss of a FYN-regulated differentiation and growth arrest pathway in advanced stage neuroblastoma. Cancer Cell 2002;2:377–86.
24. Ohira M, Morohashi A, Inuzuka H, et al. Expression profiling and characterization of 4200 genes cloned from primary neuroblastomas: identification of 305 genes differentially expressed between favorable and unfavorable subsets. Oncogene 2003;22:5525–36.
25. Ohira M, Shishikura T, Kawamoto T, et al. Hunting the subset-specific genes of neuroblastoma: expression profiling and differential screening of the full-length-enriched oligo-capping cDNA libraries. Med Pediatr Oncol 2000;35:547–9.
26. Brodeur GM, Pritchard J, Berthold F, et al. Revisions of the international criteria for neuroblastoma diagnosis, staging, and response to treatment. J Clin Oncol 1993;11:1466–77.
27. Matsumura T, Iehara T, Sawada T, Tsuchida Y. Prospective study for establishing the optimal therapy of infantile neuroblastoma in Japan. Med Pediatr Oncol 1998;31:210.
28. Kaneko M, Nishihira H, Mugishima H, et al.; Study Group of Japan for Treatment of Advanced Neuroblastoma, Tokyo, Japan. Stratification of treatment of stage 4 neuroblastoma patients based on N-*myc* amplification status. Med Pediatr Oncol 1998; 31:1–7.
29. Takihara Y, Tomotsune D, Shirai M, et al. Targeted disruption of the mouse homologue of the *Drosophila* polyhomeotic gene leads to altered anteroposterior patterning and neural crest defects. Development 1997; 124:3673–82.
30. Agulnick AD, Taira M, Breen JJ, Tanaka T, Dawid IB, Westphal H. Interactions of the LIM-domain-binding factor Ldb1 with LIM homeodomain proteins. Nature 1996;384:270–2.
31. Jurata LW, Kenny DA, Gill GN. Nuclear LIM interactor, a rhombotin and LIM homeodomain interacting protein, is expressed early in neuronal development. Proc Natl Acad Sci U S A 1996;93:11693–8.
32. Bach I, Carriere C, Ostendorff HP, Andersen B, Rosenfeld MG. A family of LIM domain-associated cofactors confer transcriptional synergism between LIM and Otx homeodomain proteins. Genes Dev 1997; 11:1370–80.
33. Osada H, Grutz G, Axelson H, Forster A, Rabbitts TH. Association of erythroid transcription factors: complexes involving the LIM protein RBTN2 and the zinc-finger protein GATA1. Proc Natl Acad Sci U S A 1995;92: 9585–9.
34. Valge-Archer VE, Osada H, Warren AJ, et al. The LIM protein RBTN2 and the basic helix-loop-helix protein TAL1 are present in a complex in erythroid cells. Proc Natl Acad Sci U S A 1994;91:8617–21.
35. Bao J, Talmage DA, Role LW, Gautier J. Regulation of neurogenesis by interactions between HEN1 and neuronal LMO proteins. Development 2000;127: 425–35.

36. Ono Y, Fukuhara N, Yoshie O. Transcriptional activity of TAL1 in T cell acute lymphoblastic leukemia (T-ALL) requires RBTN1 or -2 and induces TALLA1, a highly specific tumor marker of T-ALL. J Biol Chem 1997;272: 4576–81.
37. Aplan PD, Jones CA, Chervinsky DS, et al. An scl gene product lacking the transactivation domain induces bony abnormalities and cooperates with to generate T-cell malignancies in transgenic mice. EMBO J 1997;16:2408–19.
38. Eggert A, Grotzer MA, Ikegaki N, Liu XG, Evans AE, Brodeur GM. Expression of the neurotrophin receptor TrkA down-regulates expression and function of angiogenic stimulators in SH-SY5Y neuroblastoma cells. Cancer Res 2002;62:1802–8.
39. Ono Y, Fukuhara N, Yoshie O. TAL1 and LIM-only proteins synergistically induce retinaldehyde dehydrogenase 2 expression in T-cell acute lymphoblastic leukemia by acting as cofactors for GATA3. Mol Cell Biol 1998;18:6939–50.
40. Lutz W, Stohr M, Schurmann J, Wenzel A, Lohr A, Schwab M. Conditional expression of N-*myc* in human neuroblastoma cells increases expression of α-prothymosin and ornithine decarboxylase and accelerates progression into S-phase early after mitogenic stimulation of quiescent cells. Oncogene 1996;13:803–12.
41. Schuldiner O, Benvenisty N. A DNA microarray screen for genes involved in c-MYC and N-MYC oncogenesis in human tumors. Oncogene 2001;20:4984–94.
42. Shohet JM, Hicks MJ, Plon SE, et al. Minichromosome maintenance protein MCM7 is a direct target of the MYCN transcription factor in neuroblastoma. Cancer Res 2002;62:1123–8.

Review Article

p73, a sophisticated p53 family member in the cancer world

Toshinori Ozaki and Akira Nakagawara[1]

Division of Biochemistry, Chiba Cancer Center Research Institute, 666-2 Nitona, Chuoh-ku, Chiba 260-8717, Japan

(Received July 7, 2005/Revised August 11, 2005/Accepted August 12, 2005/Online publication October 17, 2005)

p73 belongs to a family of p53-related nuclear transcription factors that includes p53, p73 and p63. The overall structure and sequence homology indicates that a *p63/p73*-like protogene is the ancestral gene, whereas *p53* evolved later in higher organisms. In accordance with their structural similarity, p73 functions in a manner analogous to p53 by inducing tumor cell apoptosis and participating in the cell cycle checkpoint control through transactivating an overlapping set of p53/p73-target genes. In sharp contrast to p53, however, p73 is expressed as two NH_2-terminally distinct isoforms including transcriptionally active (TA) and transcriptionally inactive (ΔN) forms. ΔNp73, which has oncogenic potential, acts in a dominant negative manner against TAp73 as well as p53. p73 is induced to be stabilized in response to a subset of DNA-damaging agents in a way that is distinct from that of p53, and exerts its pro-apoptotic activity. Several lines of evidence suggest that p73 can induce tumor cell apoptosis in a p53-dependent and p53-independent manner. Some tumors exhibit resistance to the p53-dependent apoptotic program, therefore p73, which can induce apoptotic cell death by p53-independent mechanisms, is particularly useful. In this review, we discuss the regulatory mechanisms of p73 activity, and also the functional significance of p73 in the regulation of cellular processes including tumorigenesis, apoptosis and neurogenesis. (*Cancer Sci* 2005; 96: 729–737)

Until recently, the tumor suppressor p53 has been believed to be encoded by a single gene which lacks any structural or functional homologs. The identification of two p53-related proteins, termed p73 and p63, revealed that p53 belongs to a small family of sequence-specific nuclear transcription factors.[1–3] p53 family members share three major functional domains: the NH_2-terminal transactivation domain; the central core sequence-specific DNA-binding domain; and the COOH-terminal oligomerization domain. Of these, the central DNA-binding domain is highly conserved across the family. As expected from their structural similarities, p73 can bind to the p53-responsive elements, and transactivate an overlapping set of p53-target genes implicated in G1/S cell cycle arrest and apoptotic cell death.[1,4] Recent studies demonstrated that p73 is required for p53-dependent apoptosis.[5] Unlike p53, p73 is expressed as at least six variants with different COOH-terminal ends, arising from the alternative splicing at the 3′ portion of the primary transcript.[1,6,7] Each of these splicing variants (TAp73) contains an intact NH_2-terminal transactivation domain, and exerts its transcriptional activity to various degrees. Additionally, *p73* contains a second transcriptional start site within intron 3, giving rise to the NH_2-terminally truncated form of p73 (ΔNp73) which has little transcriptional activity.[8] Similar to p73, ΔNp63 is also generated by an alternative promoter (Fig. 1a,b).[2] ΔNp73 displays dominant negative behavior toward p73 as well as wild-type p53, and has oncogenic potential.[9,10] Of note, we and others found that ΔNp73 is a direct transcriptional target of p73, suggesting that there exists a negative feedback regulation of p73 by ΔNp73, to modulate cell survival and death.[11–13]

Steady-state expression levels of endogenous p73 are kept extremely low under physiological conditions. Similar to p53, p73 is induced to be stabilized at the protein level in response to a subset of DNA-damaging agents, and exerts its pro-apoptotic activity.[14] Accumulating evidence suggests that p73 turnover is regulated through a ubiquitination-dependent and ubiquitination-independent degradation pathway. MDM2 acts as an E3 ubiquitin protein ligase for p53, and promotes the proteasome-mediated proteolytic degradation of p53.[15–17] On the other hand, MDM2 increases the stability of p73,[18] indicating that p73 stability is regulated through a pathway distinct from that of p53. Alternatively, Ohtsuka *et al.* reported that cyclin G binds to p73 and stimulates its proteolytic degradation in a ubiquitination-independent manner, however, the precise molecular mechanism of cyclin G-mediated degradation of p73 remains unknown.[19]

Considering that p73 has a p53-like property and is mapped to the human chromosome 1p36.2-3, a region which is frequently lost in a wide variety of human tumors including neuroblastoma, it is likely that p73 could be one of the classic Knudson-type tumor suppressors.[1] In spite of extensive mutation searches, *p73* was rarely mutated in primary tumors.[20] Additionally, initial genetic studies demonstrated that p73-deficient mice exhibit severe developmental defects, however, they do not develop spontaneous tumors, suggesting that p73 might participate in the regulation of normal development *in vivo*, and that p73 does not link directly to tumor suppression.[8] Indeed, p73 has the ability to induce neuronal differentiation of undifferentiated neuroblastoma cells.[21] However, this viewpoint has been challenged by the observation that mice mutant for p73 and p63 develop spontaneous tumors, and their spectrum is quite different from that of p53-deficient mice.[22] Thus, it is likely that p73 and

[1]To whom correspondence should be addressed. E-mail: akiranak@chiba-cc.jp

Abbreviations: EEC, ectrodactyly, ectodermal dysplasia, and facial clefts (syndrome); OPC, oligodendrocyte precursor cell; SAM, sterile α motif; YAP, Yes-associated protein.

 doi: 10.1111/j.1349-7006.2005.00116.x

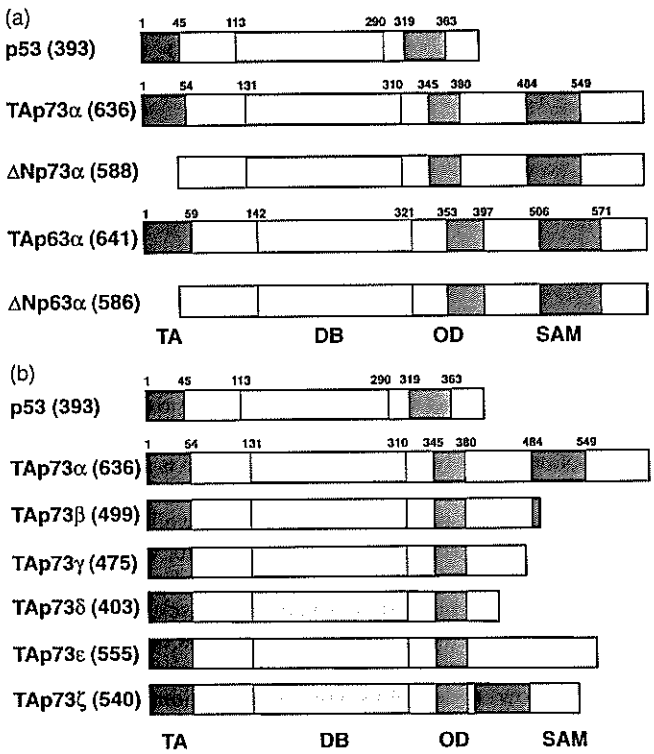

Fig. 1. (a) Structural comparison between TA and ΔN variants. The transactivation domain (TA), DNA-binding domain (DB), oligomerization domain (OD) and sterile α motif domain (SAM) are indicated. ΔN variant, which lacks the NH_2-terminal transactivation domain, is generated by alternative promoter usage. The numbers in parentheses are the amino acid lengths of each protein. (b) Schematic drawing of the splicing variants of p73. p73 is expressed as multiple variants with different COOH-terminal ends arising from an alternative splicing at the 3′ portion of the primary transcript. The numbers in parentheses are the amino acid lengths of each protein.

p63 exert their tumor suppressor activity in specific tissues. In this review, we will discuss the functional significance of p73 in the regulation of cellular processes such as tumorigenesis, apoptotic cell death and neuronal differentiation.

Splicing variants of p73

The overall genomic organization of *p73* is quite similar to that of *p53*. The *p53* gene is 20 kb in length and contains 11 exons. The *p73* gene is larger than 60 kb in length and contains 14 exons.[23] In sharp contrast to p53, p73 is expressed as multiple variants arising from an alternative splicing of the primary *p73* transcript including p73α, p73β, p73γ, p73δ, p73ε, and p73ζ.[1,6,7] Among them, p73α is the longest form, which contains a sterile α motif domain (SAM domain) and an extreme COOH-terminal region, whereas p73β lacks the extreme COOH-terminal tail and most of the SAM domain. We and others revealed that these COOH-terminal splicing variants display different transcriptional and biological properties.[6,7,24] Indeed, the ability of p73β to transactivate a variety of p53/p73 target genes and to induce apoptotic cell death in certain cancerous cells was stronger than those of the full-length p73α.[7,25] This indicated that the COOH-terminal region of p73 might possess a regulatory role, which modulates its transcriptional and pro-apoptotic activity[24,25] These splicing variants with different COOH-terminal extensions were expressed differentially among normal human tissues and cell lines, suggesting that they have distinct physiological functions.[6,7]

TAp73 and ΔNp73

In addition to the differential splicing variants of p73, there exist the ΔN variant forms of p73 (ΔNp73α and ΔNp73β) which are transcribed from an internal promoter located within an extra exon (exon 3′) of the full-length *p73* gene, and lacks the NH_2-terminal transactivation domain in TAp73.[8] Like p73, ΔNp63 is also generated using an alternative promoter.[2] As expected, ΔNp73 has little transactivation activity. Furthermore, ΔNp73 displays dominant negative behavior toward TAp73 as well as wild-type p53,[9] and also has oncogenic potential.[10] ΔNp73-mediated inhibition of TAp73 and p53 occurs at the oligomerization level or by the competition for binding to the same p53/p73-responsive element, with ΔNp73 displacing TAp73 and p53 from the DNA binding site.[26,27] For example, ΔNp73 was expressed predominantly in sympathetic neurons, and inhibited p53-dependent neuronal apoptosis.[9] ΔNp73-dependent repression of apoptosis induced by p53 is critical for the normal development of the neural system. In addition, the endogenous expression levels of ΔNp73 were significantly associated with poor prognosis in human cancers such as neuroblastoma.[28] Thus, it is likely that a balance between the intracellular expression levels of pro-apoptotic TAp73 or p53 and anti-apoptotic ΔNp73 plays an important role in regulating cell fate determination. Intriguingly, we and others demonstrated that there exists a functional p53/p73-responsive element within the *ΔNp73* promoter region, and indeed the expression of ΔNp73 is directly transactivated by TAp73 and/or wild-type p53, creating a dominant negative feedback loop which regulates the pro-apoptotic activities of both TAp73 and wild-type p53[11–13] (Fig. 2).

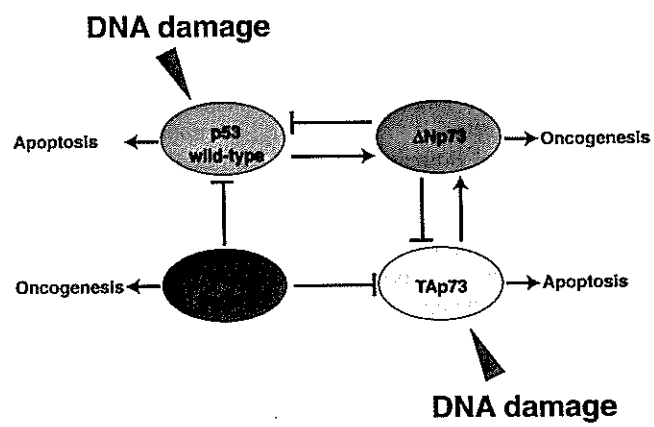

Fig. 2. Functional interactions between TAp73, ΔNp73, wild-type p53 and a mutant form of p53. DNA damage induces TAp73 and wild-type p53 through distinct pathways. The mutant form of p53 inhibits the pro-apoptotic activity of TAp73 and wild-type p53. ΔNp73, which is directly transactivated by TAp73 and wild-type p53, displays dominant negative behavior toward TAp73 and wild-type p53.

 doi: 10.1111/j.1349-7006.2005.00116.x

As described above, ΔNp73 is transcriptionally inactive due to a lack of the NH_2-terminal transactivation domain in TAp73. However, this viewpoint has been challenged by the recent finding of Liu *et al.* showing that ΔNp73β has weak but distinct transcriptional activity, thereby inducing cell cycle arrest and/or apoptosis.[29] In contrast to ΔNp73β, ΔNp73α failed to induce cell cycle arrest and/or apoptosis under their experimental conditions. According to their results, the NH_2-terminal 13 unique amino acid residues as well as PXXP motifs of ΔNp73β might be a novel activation domain. Thus, it is possible that ΔNp73β might exert a distinct function under certain cellular processes.

Transcriptional regulation of the main promoter of p73

E2F1 transcription factor plays an important role in the regulation of cell cycle progression by inducing the transcription of genes whose products are directly or indirectly required for entry into the S phase.[30] In addition to the proliferative effect of deregulated E2F1 activity, unscheduled E2F1 activation leads to apoptosis to protect cells from cellular transformation.[31] Consistent with this notion, E2F1-deficient mice exhibited a high incidence of unusual tumors.[32,33] E2F1-induced apoptosis is regulated in a p53-dependent or p53-independent manner. It is interesting that the *p73* promoter region contains a TATA-like box and at least three E2F1-binding sites, and indeed the enforced expression of E2F1 strongly stimulates the transcription of *p73* through the direct binding to the E2F1-responsive elements in the *p73* promoter.[34,35] The E2F1-mediated up-regulation of p73 results in a significant induction of apoptosis. Other studies demonstrated that T cell receptor-mediated apoptosis is dependent on both E2F1 and p73.[36] Thus, E2F1-mediated apoptosis requires p73, at least in part. Alternatively, E2F1 might also contribute to the up-regulation of *p73* mRNA levels during muscle and neuronal differentiation of murine C2C12 myoblasts and P19 cells, respectively.[37] It is worth noting that Chk1 and Chk2 are required for the induction of p73 in response to DNA damage, and E2F1 contributes to the Chk kinase-dependent transcriptional regulation of p73.[38] In addition to E2F1, cellular and viral oncogene products such as c-Myc and E1A indirectly activated the transcription of p73.[39]

Recently, Fontemaggi *et al.* identified a 1 kb negative regulatory fragment within the first intron of *p73* gene.[37] Under their experimental conditions, this intronic fragment significantly reduced the activity of the *p73* promoter upon E2F1 overexpression. Of note, the *p73* intronic fragment contained six consensus binding sites for transcriptional repressor ZEB. Ectopic expression of ZEB in C2C12 myoblasts attenuated myotube formation, and repressed the transcription of *p73*. In accordance with these results, the dominant negative form of ZEB had an ability to restore the expression levels of p73 in proliferating cells.

Because DNA hypermethylation contributes to the alteration of the entry of transcription factors into the regulatory region, the epigenetic modification of the *p73* promoter region through aberrant hypermethylation could be an alternative molecular mechanism for silencing the *p73* gene. Corn *et al.* described the aberrant promoter methylation of *p73* as occurring frequently in primary acute lymphoblastic leukemias and Burkitt's lymphomas, whereas the *p73* promoter methylation was not detected in normal lymphocytes or bone marrow.[40] Similar results were also reported by Kawano *et al.*[41] In contrast, hypermethylation of the *p73* promoter region was not observed in solid tumors including breast, renal, colon cancers or neuroblastomas,[42] suggesting that the methylation-dependent silencing of *p73* transcription might be specific to hematological malignancies.

p73 is rarely mutated in human cancers

The *p73* gene has been mapped to human chromosome 1p36.2-3, a region which exhibits frequent loss of heterozygosity in a wide variety of human cancers including neuroblastoma, and its gene product has an ability to promote G1/S cell cycle arrest and/or cell death through apoptosis in certain cancerous cells. Therefore, p73 could act as a tumor suppressor.[1] In spite of an extensive search of the *p73* status in human primary tumors, *p73* was infrequently mutated in many human tumors.[20,43–48] *p73* mutations were detected in fewer than 0.5% of human cancers, whereas over 50% of cancers carry *p53* mutations. For example, only two types of *p73* mutations with amino acid substitution (P405R and P425L) were found in primary neuroblastoma and lung cancer.[20] In addition to the NH_2-terminal transactivation domain, Takada *et al.* found a potential second transactivation domain within the COOH-terminal portion of p73α (amino acid residues 380–513), albeit to a lesser extent than the NH_2-terminal transactivation domain.[49] This region is rich in glutamine and proline residues. Among the two types of p73 mutations, the P425L substitution significantly reduced the transcriptional and growth-suppressive activity of p73α, whereas the P405R substitution had a negligible effect on p73α.[50]

In sharp contrast to p53-deficient mice, which develop tumors with high frequency,[51] p73-deficient mice were viable, but the loss of p73 did not predispose mice to cancer, suggesting that p73 does not function as a classic Knudson-type tumor suppressor,[8] and its possible contribution to tumor suppression is still unclear. Instead, mice lacking p73 displayed severe developmental defects, including hydrocephalus, hippocampal dysgenesis, and abnormalities in the pheromone sensory pathways. These observations strongly suggest that p73 and p53 have distinct biological functions, and p73 plays an important role in normal development, especially in neural development and apoptosis. Because those p73-deficient mice lacked both TAp73 and ΔNp73 variants, further studies of variant-specific knockout mice might provide an insight into the unique role of each variant in tumorigenesis.

As mentioned above, initial genetic studies revealed that p73-deficient mice do not display an increased susceptibility to spontaneous tumorigenesis. More recently, Flores *et al.* examined whether synergistic effects of p73 and p63 could exist, alone or in combination with p53, in tumor suppression.[22] Strikingly, they found that p73 and p63 heterozygous mice ($p73^{+/-}$ and $p63^{+/-}$) developed malignant tumors at high frequency including various tumor types not observed in $p53^{+/-}$ mice, and $p53^{+/-}$; $p73^{+/-}$ and $p53^{+/-}$; $p63^{+/-}$ mice

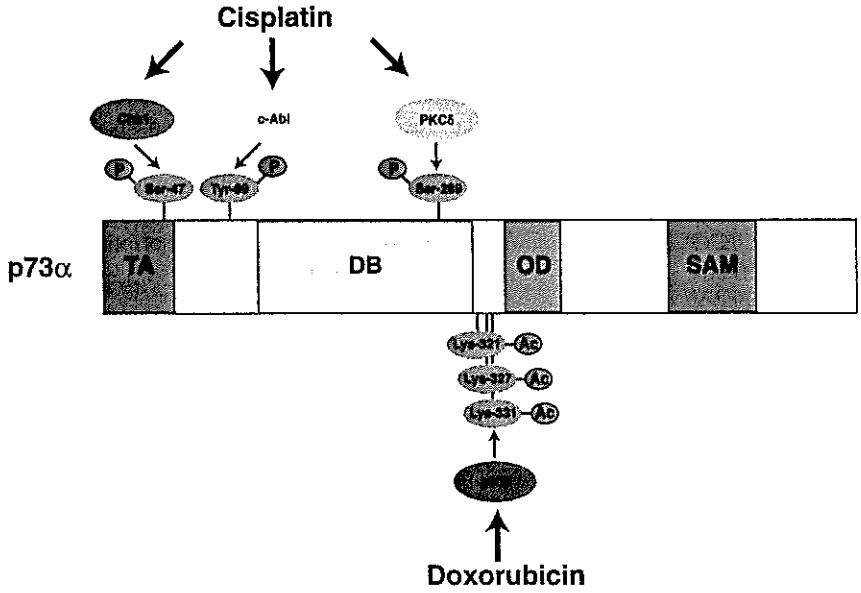

Fig. 3. DNA damage-induced activation of p73 is mediated by post-translational modifications including phosphorylation and acetylation. During cisplatin-mediated apoptosis, p73 is induced to be phosphorylated at Ser-47, Tyr-99 and Ser-289 by Chk1, c-Abl and PKCδ, respectively. In response to doxorubicin, p300 acetylates p73 at Lys-321, Lys-327 and Lys-331.

developed a more aggressive tumor phenotype.[22] In addition, tumors derived from $p73^{+/-}$ and $p63^{+/-}$ mice exhibited loss of the remaining wild-type allele at high frequency. These results strongly suggest that loss of p73 and/or p63 function causes tumor development, and their tumor suppressor activities play a pivotal role in specific tissues distinct from those of p53.

Activation of p73 at protein level by genotoxic stresses

Under normal physiological conditions, the expression levels of the p73 protein are maintained at an extremely low level, keeping this pro-apoptotic protein in an inactive state. The initial studies demonstrated that, unlike p53, p73 is not induced at the protein level in response to DNA damage.[1] Indeed, the exposure to either actinomycin D or ultraviolet radiation had no significant effects on p73 protein levels, whereas p53 and one of its target $p21^{WAF1}$ levels were markedly elevated in response to actinomycin D or ultraviolet radiation. However, recent studies revealed that p73 is induced to be accumulated in response to a subset of DNA-damaging agents, including cisplatin, adriamycin, camptothecin and etoposide.[14] p73 is predominantly regulated at the post-translational level, and the stabilization of p73 results in either G1/S cell cycle arrest or cell death through apoptosis. Therefore, the stabilization of p73 is directly linked with its activity.

Accumulating evidence strongly suggests that chemical modifications of p73, such as phosphorylation and acetylation, prolong its half-life, which, in turn, enhance its transcriptional and pro-apoptotic activity. During the cisplatin-mediated apoptotic process, p73 is phosphorylated at Tyr-99 and stabilized in a pathway dependent on nuclear non-receptor tyrosine kinase c-Abl.[52–54] In addition to c-Abl, exposure to cisplatin promoted a complex formation between p73 and a protein kinase Cδ catalytic fragment, which phosphorylated p73 at Ser-289 and increased its stability and transcriptional activity.[55] Recently, it has been shown that cisplatin-induced apoptosis is associated with p73 phosphorylation at Ser-47 mediated by Chk1.[56] Chk1-dependent phosphorylation resulted in an increase in the transcriptional activity of p73 (Fig. 3). In contrast, CDK-mediated phosphorylation of p73 led to significant inhibition of its transcriptional activity,[57] indicating that the phosphorylation of p73 might not always convert a latent form of p73 to an active one.

Alternatively, p73 is regulated by acetylation. p73 was previously found to be associated with p300 histone acetyltransferase through its NH_2-terminal transactivation domain, and this interaction resulted in a significant enhancement of p73-mediated transcriptional activation as well as apoptosis.[58] Costanzo *et al.* reported that p300 acetylates p73 at Lys-321, Lys-327 and Lys-331 in response to doxorubicin in a c-Abl-dependent manner, and the acetylated forms of p73 have pro-apoptotic activity[59] (Fig. 3). Intriguingly, the p300-mediated acetylation of p73 was stimulated by prolyl isomerase Pin1, thereby stabilizing p73.[60] It is likely that p73 acetylation catalyzed by p300 reduces its ubiquitination levels by competition between acetylation and ubiquitination.

Regulation of p73 turnover

Lee and La Thangue described p73 as being stabilized in cells treated with proteasome inhibitor such as LLnL.[25] They also showed that p73β is much more stable than p73α, indicating that the COOH-terminal extension of p73α might be involved in the stability control of p73. In support of this notion, we have found that RanBPM binds to the extreme COOH-terminal region of p73α, and prolongs the half-life of p73α.[61] Subsequently, several lines of evidence suggest that p73 turnover is regulated by a ubiquitination-dependent and a ubiquitination-independent proteasome pathway. MDM2, which is transcriptionally activated by p53, acts as an E3 ubiquitin protein ligase for p53. MDM2 promotes the ubiquitination of p53 through physical interaction with its

 doi: 10.1111/j.1349-7006.2005.00116.x

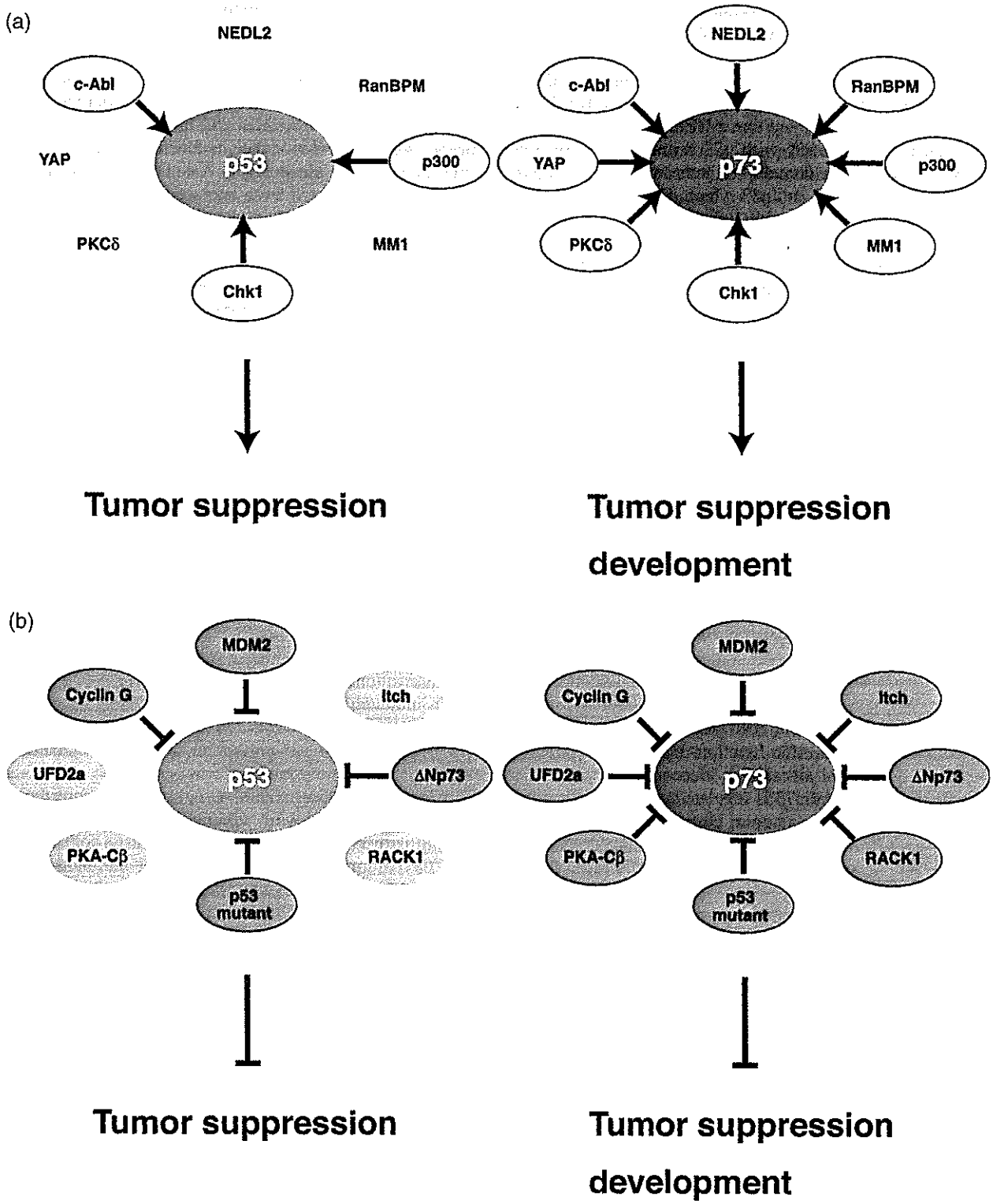

Fig. 4. Positive (a) and negative (b) regulation of p73 or p53 activity through the physical and functional interaction with various cellular proteins. Uncircled proteins have an undetectable effect on p53.

NH_2-terminal transactivation domain, and subsequent proteolytic degradation of p53.[15–17] Similar to p53, MDM2 was also a direct transcriptional target of p73, bound to its NH_2-terminal transactivation domain and thereby inhibiting p73-mediated transcriptional activation and apoptosis. However, MDM2 failed to ubiquitinate p73, and this interaction resulted in an increase in p73 protein stability.[18] Additionally, a newly identified p53-induced E3 ubiquitin

protein ligase Pirh2, which stimulates the ubiquitination-dependent proteolytic degradation of p53, had a negligible effect on p73.[62,63] These observations strongly indicate that p73 turnover is regulated by an as yet unidentified E3 ubiquitin protein ligase(s) distinct from that used for p53.

Recently, Rossi *et al.* found that a HECT-type E3 ubiquitin protein ligase Itch interacts with p73 through the WW protein–protein interaction domains of Itch and the p73 region containing the PY motif, and p53 which does not contain the PY motif fails to interact with Itch.[64] According to these results, Itch had an ability to ubiquitinate and degrade p73. Upon DNA damage induced by chemotherapeutic drugs including cisplatin, doxorubicin or etoposide, the endogenous expression levels of Itch were significantly down-regulated through an unknown mechanism, thereby increasing the stability and activity of p73. On the other hand, we have found that a novel HECT-type E3 ubiquitin protein ligase NEDL2 directly binds to p73, and this interaction is mediated by the WW domains of NEDL2 and the COOH-terminal region of p73 containing the PY motif.[65] Unexpectedly, NEDL2 promoted the ubiquitination of p73 in cells, however, NEDL2-mediated ubiquitination increased the stability of p73 and enhanced the p73-dependent transcriptional activation, indicating that there exists a non-proteolytic regulatory role of ubiquitination. Other studies demonstrated that the NH_2-terminally truncated form of p73 (ΔNp73) is much more stable than TAp73, suggesting that p73-mediated transcriptional activation is required for the rapid turnover of p73, and that, like p53, one or more transcriptional targets of p73 might promote its proteolytic degradation.[63] Additionally, Toh *et al.* reported that c-Jun increases the stability of p73 without direct interaction, and c-Jun-mediated stabilization of p73 is regulated in its transactivation function-dependent manner.[66]

Alternatively, several lines of evidence suggest that the proteolytic degradation of p73 is regulated in a ubiquitination-independent manner. For example, Ohtsuka *et al.* found that cyclin G, one of the direct transcriptional targets of p53 and p73, interacts with p73 and induces the latter's rapid degradation.[19] According to these results, cyclin G-mediated degradation of p73 was not associated with an increase in its ubiquitination levels. Recently, we have demonstrated that a U-box-type E3/E4 ubiquitin protein ligase UFD2a interacts with p73 through its COOH-terminal SAM domain, and induces the proteasomal turnover of p73.[67] Intrinsic E3/E4 ubiquitin protein ligase activity was not necessary for the UFD2a-mediated proteolytic degradation of p73, and UFD2a failed to increase the ubiquitination levels of p73. Similar to Itch, the intracellular expression levels of UFD2a were significantly down-regulated at protein levels in response to cisplatin, thereby leading to a dissociation of free active p73 from the p73/UFD2a complex. Although the precise molecular mechanisms underlying the proteasome-dependent degradation of p73 mediated by UFD2a are not yet known, it is likely that p73 might be recruited to the proteasome through its interaction with UFD2a.

Molecules interacting with p73

In addition to post-translational modifications including phosphorylation and acetylation, the activity of p73 is regulated by physical interaction with several viral and cellular proteins. As p53 and p73 share the same domain organization, consisting of the NH_2-terminal transactivation domain, the central sequence-specific DNA-binding domain and the COOH-terminal oligomelization domain, initial studies were performed to examine whether p53-binding proteins could also interact with p73 and modulate its function. Like p53, p73 was associated with the adenovirus E1A and the T-cell lymphotropic virus I-derived Tax, and these interactions inhibited the activity of p73.[23] On the other hand, the viral proteins which can bind to and inactivate p53, including the adenovirus E1B, papilomavirus E6 and simian virus 40 T antigen, failed to interact with p73.[68–70] For cellular proteins, MDM2 interacted with both p53 and p73, and inactivated their activities.[18,71]

Recently, several experimental approaches have been employed to identify the specific binding partners of p73. We and others focussed attention on the PY motif of p73 not found in p53, and identified the Yes-associated protein (YAP), NEDL2 and Itch.[64,65,72] As mentioned above, NEDL2 ubiquitinated p73 but extended its half-life, thereby enhancing its transcriptional activation. Itch promoted the ubiquitination-mediated proteasomal turnover of p73. YAP interacted with the PY motif of p73 through its WW domain, and stimulated p73-mediated transcriptional activation. We performed a conventional yeast-based two-hybrid screening using the extreme COOH-terminal tail of p73 not found in p53. Finally, we identified the c-Myc-binding protein (MM1), RACK1 and RanBPM as p73-binding proteins.[61,73,74] Based on our results, MM1 attenuated the c-Myc-mediated inhibition of transcriptional activity of p73, whereas RACK1 significantly inhibited the function of p73 and its inhibitory effect was counteracted by pRB. RanBPM increased the stability of p73 by reducing its ubiquitination levels. The proteins we identified had no detectable effects on p53. By using a new CytoTrap yeast two-hybrid screening, we identified the protein kinase A catalytic subunit β (PKA-Cβ) as a novel binding partner of p73.[75] PKA-Cβ bound to both the NH_2- and COOH-terminal regions of p73, and inhibited its transcriptional activity. PKA-Cβ efficiently phosphorylated p73, and PKA-Cβ-mediated inhibition of p73 was dependent on the kinase activity of PKA-Cβ (Fig. 4a,b). These observations strongly suggest that the regulatory mechanisms of p73 are distinct from those of p53.

Mutual regulation between p73 and p53

Previously, it has been shown that tumor-derived p53 mutants but not wild-type p53 interact with p73, and abrogate its function.[76] Subsequent studies demonstrated that the ability of p53 mutants to interact with p73 depends on the nature of the p53 mutations as well as the polymorphism at codon 72 (Pro-72 or Arg-72) of p53 mutants.[77] According to their results, p53 mutants carrying Arg-72 bound to p73 better than p53 mutants with Pro-72. Consistent with this notion, p53 mutants carrying Arg-72 act as more potent inhibitors of chemotherapy-induced apoptosis than the p53 mutants with Pro-72.[78] Other studies focused on the functional interaction between wild-type p53 and p73. Miro-Mur *et al.* reported that p73 induces both accumulation and activation of wild-type p53 by preventing MDM2-mediated degradation

 doi: 10.1111/j.1349-7006.2005.00116.x

through MDM2 titration.[79] In addition, Goldschneider *et al.* found that p73 promotes the nuclear localization of wild-type p53 in neuroblastoma cells in which p53 is predominantly expressed in cytoplasm.[80] These results suggest that p73 has an ability to enhance the activity of wild-type p53. In contrast, Vikhanskaya *et al.* described that p73 reduces the p53-mediated transcriptional activation through the competition of the same DNA-binding site.[81] These controversial results regarding the effects of p73 on wild-type p53 might be at least in part due to the different cell systems used in those studies.

Recently, it has been shown that p53-dependent apoptosis requires the indirect contribution of at least one other p53 family member, p73 or p63.[5] Thus, it is likely that p73 cooperates with p53 to promote apoptotic cell death. These findings emphasize the functional importance of p73 in the regulation of the DNA damage-induced apoptotic response.

Role of p73 in neuronal differentiation

Considering that p73-deficient mice in which both TAp73 and ΔNp73 have been deleted, displayed profound developmental defects in their nervous and immune systems including a severe distortion of the hippocampal formation, it is likely that p73 contributes to normal neural development.[8] Indeed, ΔNp73 was expressed predominantly in the developing brain and sympathetic neurons, and p53-dependent neuronal apoptosis was inhibited by ΔNp73.[9] Consistent with this notion, De Laurenzi *et al.* demonstrated that p73 is induced to be accumulated during retinoic acid-mediated neuronal differentiation in neuroblastoma cell lines, whereas p53 levels remained unchanged in response to retinoic acid.[21] Under their experimental conditions, ectopic overexpression of p73 in undifferentiated neuroblastoma cell lines resulted in the induction of neurite extension as well as the expression of neuronal differentiation markers. In contrast, the transcriptionally inactive mutant form of p73 had undetectable effects on the neuronal differentiation. Similar results were also observed during neuronal differentiation in P19 cells exposed to retinoic acid.[46] Of note, Billon *et al.* described that the ectopic expression of p73 induces oligodendrocyte precursor cell (OPC) differentiation, and that ΔNp73 inhibits OPC differentiation in culture.[82] These observations strongly suggest that, in addition to its apoptosis-inducing activity upon DNA damage, p73 plays a pivotal role in the regulation of proper neuronal differentiation.

Role of p73 in the p53-independent cellular pathway

p53 plays a central role in the regulation of apoptotic cell death in response to DNA damaging agents. p53 function is lost by various mechanisms, including loss of function mutations within the *p53* gene itself or defects in upstream and/or downstream mediators of p53. Recent findings clearly demonstrated that p53-dependent apoptosis in response to DNA damage is impaired in cells lacking both p73 and p63, indicating that p73 and p63 are critical components of the apoptotic response to DNA damage.[5] Accumulating evidence strongly suggests that the pro-apoptotic activity of p73 is regulated through a pathway distinct from that used for p53. As certain cancerous cells were resistant to p53-dependent apoptotic cell death, p73 could be one of several candidate tumor suppressor proteins which can promote apoptosis by p53-independent mechanisms. Previous studies revealed that the exogenous expression of p73 in p53-deficient cells results in significant cell death through apoptosis in a p53-independent manner.[4] It is worth noting that p73 has an ability to promote apoptotic cell death in various pancreatic cells lacking functional p53, which are resistant to wild-type p53 gene transfer.[83] Thus, it is possible that p73 could be particularly useful in treating cancerous cells with non-functional p53.

What is the difference between p73 and p63?

The overall genomic organization of *p63* is quite similar to that of *p73*; the *p63* gene contains 15 exons.[23] Although *p63* is mapped to human chromosome 3q27–29, a region which is altered in a variety of cancers derived from lung, cervix or ovary, *p63* was infrequently mutated in primary tumors.[2,20] Like p73, p63 gives rise to at least six splicing variants as well as an NH_2-terminally truncated form of p63 (ΔNp63) arising from the alternative promoter usage. ΔNp63, a direct transcriptional target of p53, had a dominant negative effect on TAp63.[84] As expected from its structural similarity to p73, p63 can bind to the p53-responsive element and transactivate an overlapping set of p53-regulated genes, thereby inducing cell cycle arrest and/or apoptosis.[2] In contrast to p73, E2F1 did not stimulate the transcription of *p63*, although the putative E2F1-binding sites were found within the *p63* promoter region.[84]

At a sequence level, *p63* is much more similar to *p73* than *p53*, raising the possibility that *p73* or *p63* might be the original *p53* family gene, and that *p53* might be phylogenetically younger.[85] In support of this notion, p73 and p63 contribute to normal development, and p53 holds additional biological properties such as strong tumor suppressor activity. Despite the structural and functional similarities between p73 and p63, knockout phenotypes and the expression patterns of p63 were quite different from those of p73. In sharp contrast to *p73*, whose expression was restricted to the epidermis, sinuses, inner ear and brain, *p63* was predominantly expressed in the epidermis, cervix, urothelium and prostate.[23] Unlike p73-deficient mice, p63-deficient mice exhibited severe defects in limb, cranio-facial and epithelial development.[86,87] For example, p63-deficient mice lacked all squamous epithelia, and displayed severe forelimb truncations. Consistent with these developmental defects, *p63* mutations were detected in children affected by EEC (ectrodactyly, ectodermal dysplasia, and facial clefts) syndrome.[88] Thus, it is likely that p73 and p63 have overlapping and distinct biological activities, and they express their specific functions depending on their unique sites of action.

Conclusion

p53 and p73 share extensive structural and functional similarities. They have overlapping as well as distinct biological functions. In addition to its potent tumor suppressor function, at least in specific tissues, p73 plays a pivotal role in normal neurogenesis *in vivo*. Similar to

p53, p73 is induced to be accumulated in response to a subset of DNA-damaging agents, however, the regulatory mechanisms of the pro-apoptotic activity of p73 are distinct from those used for p53. p73 has the ability to induce apoptotic cell death in a p53-independent manner. Indeed, p73 can promote apoptotic cell death in tumor cells that lack functional p53. In addition, p73 might enhance the chemosensitivity of tumor cells. Therefore, p73 alone or in combination with the other p53 family members might provide a clue to overcoming chemoresistance in tumor cells.

References

1 Kaghad M, Bonnet H, Yang A *et al.* Monoallelically expressed gene related to p53 at 1p36, a region frequently deleted in neuroblastoma and other human cancers. *Cell* 1997; **90**: 809–19.
2 Yang A, Kaghad M, Wang Y *et al.* p63, a p53 homolog at 3q27–29, encodes multiple products with transactivation, death-inducing, and dominant-negative activities. *Mol Cell* 1998; **2**: 305–16.
3 Osada M, Ohba M, Kawahara C *et al.* Cloning and functional analysis of human p51, which structurally and functionally resembles p53. *Nat Med* 1998; **4**: 839–43.
4 Jost CA, Marin MC, Kaelin WG Jr. p73 is a simian p53-related protein that can induce apoptosis. *Nature* 1997; **389**: 191–4.
5 Flores ER, Tsai KY, Crowley D *et al.* p63 and p73 are required for p53-dependent apoptosis in response to DNA damage. *Nature* 2002; **416**: 560–4.
6 De Laurenzi V, Costanzo A, Barcaroli D *et al.* Two new p73 splice variants, γ and δ, with different transcriptional activity. *J Exp Med* 1998; **188**: 1763–8.
7 Ueda Y, Hijikata M, Takagi S, Chiba T, Shimotohno K. New p73 variants with altered C-terminal structures have varied transcriptional activities. *Oncogene* 1999; **18**: 4993–8.
8 Yang A, Walker N, Bronson R *et al.* p73-deficient mice have neurological, pheromonal and inflammatory defects but lack spontaneous tumours. *Nature* 2000; **404**: 99–103.
9 Pozniak CD, Radinovic S, Yang A, Mckeon F, Kaplan DR, Miller FD. An anti-apoptotic role for the p53 family member, p73, during developmental neuron death. *Science* 2000; **289**: 304–6.
10 Stiewe T, Zimmermann S, Frilling A, Esche H, Putzer BM. Transactivation-deficient ΔTA-p73 acts as an oncogene. *Cancer Res* 2002; **62**: 3598–602.
11 Grob TJ, Novak U, Maisse C *et al.* Human ΔNp73 regulates a dominant negative feedback loop for TAp73 and p53. *Cell Death Differ* 2001; **8**: 1213–23.
12 Nakagawa T, Takahashi M, Ozaki T *et al.* Autoinhibitory regulation of p73 by ΔNp73 to modulate cell survival and death through a p73-specific target element within the ΔNp73 promoter. *Mol Cell Biol* 2002; **22**: 2575–85.
13 Zaika AI, Slade N, Erster SH *et al.* ΔNp73, a dominant-negative inhibitor of wild-type p53 and TAp73, is up-regulated in human tumors. *J Exp Med* 2002; **196**: 765–80.
14 Irwin MS, Kondo K, Marin MC *et al.* Chemosensitivity linked to p73 function. *Cancer Cell* 2003; **3**: 403–10.
15 Haupt Y, Maya R, Kazaz A, Oren M. MDM2 promotes the rapid degradation of p53. *Nature* 1977; **387**: 296–9.
16 Kubbutat MHG, Jones SN, Vousden KH. Regulation of p53 stability by MDM2. *Nature* 1997; **387**: 299–303.
17 Honda R, Tanaka H, Yasuda H. Oncoprotein MDM2 is a ubiquitin ligase E3 for tumor suppressor p53. *FEBS Lett* 1997; **420**: 25–7.
18 Zeng X, Chen L, Jost CA *et al.* MDM2 suppresses p73 function without promoting p73 degradation. *Mol Cell Biol* 1999; **19**: 3257–66.
19 Ohtsuka T, Ryu H, Minamishima YA, Ryo A, Lee SW. Modulation of p53 and p73 levels by cyclin G: Implication of a negative feedback regulation. *Oncogene* 2003; **22**: 1678–87.
20 Ikawa S, Nakagawara A, Ikawa Y. p53 family genes: Structural comparison, expression and mutation. *Cell Death Differ* 1999; **6**: 1154–61.
21 De Laurenzi V, Raschella G, Barcaroli D *et al.* Induction of neuronal differentiation by p73, in a neuroblastoma cell line. *J Biol Chem* 2000; **275**: 15226–31.
22 Flores ER, Sengupta S, Miller JB *et al.* Tumor predisposition in mice mutant for p63 and p73: Evidence for broader tumor suppressor functions for the p53 family. *Cancer Cell* 2005; **7**: 363–73.
23 Irwin MS, Kaelin WG Jr. p53 family update: p73 and p63 develop their own identities. *Cell Growth Differ* 2001; **12**: 337–49.
24 Ozaki T, Naka M, Takada N *et al.* Deletion of COOH-terminal region of p73α enhances both its transactivation function and DNA-binding activity but inhibits induction of apoptosis in mammalian cells. *Cancer Res* 1999; **59**: 5902–7.
25 Lee C-W, La Thangue NB. Promoter specificity and stability control of the p53-related protein p73. *Oncogene* 1999; **18**: 4171–81.
26 Stiewe T, Theseling CC, Putzer BM. Transactivation-deficient ΔTA-p73 inhibits p53 by direct competition for DNA binding. *J Biol Chem* 2002; **277**: 14177–85.
27 Melino G, De Laurenzi V, Vousden KH. p73: Friend or foe in tumorigenesis. *Nat Rev Cancer* 2002; **2**: 605–15.
28 Casciano I, Mazzocco K, Boni L *et al.* Expression of ΔNp73 is a molecular marker for adverse outcome in neuroblastoma patients. *Cell Death Differ* 2002; **9**: 246–51.
29 Liu G, Nozell S, Xiao H, Chen X. ΔNp73β is active in transactivation and growth suppression. *Mol Cell Biol* 2004; **24**: 487–501.
30 Johnson DG, Schwarz JK, Cress WD, Nevins JR. Expression of transcription factor E2F1 induces quiescent cells to enter S phase. *Nature* 1993; **365**: 349–52.
31 Shan B, Lee W-H. Deregulated expression of E2F-1 induces S-phase entry and leads to apoptosis. *Mol Cell Biol* 1994; **14**: 8166–73.
32 Yamasaki L, Jacks T, Bronson R, Goillot E, Harlow E, Dyson NJ. Tumor induction and tissue atrophy in mice lacking E2F-1. *Cell* 1996; **85**: 537–48.
33 Field SJ, Tsai F-Y, Kuo F *et al.* E2F-1 functions in mice to promote apoptosis and suppress proliferation. *Cell* 1996; **85**: 549–61.
34 Irwin M, Marin MC, Phillips AC *et al.* Role for the p53 homologue p73 in E2F-1-induced apoptosis. *Nature* 2000; **407**: 645–8.
35 Stiewe T, Putzer BM. Role of the p53-homologue p73 in E2F1-induced apoptosis. *Nat Genet* 2000; **26**: 464–9.
36 Lissy NA, Davis PK, Irwin M, Kaelin WG Jr, Dowdy SF. A common E2F-1 and p73 pathway mediates cell death induced by TCR activation. *Nature* 2000; **407**: 642–5.
37 Fontemaggi G, Gurtner A, Strano S *et al.* The transcriptional repressor ZEB regulates p73 expression at the crossroad between proliferation and differentiation. *Mol Cell Biol* 2001; **21**: 8461–70.
38 Urist M, Tanaka T, Poyurovsky MV, Prives C. p73 induction after DNA damage is regulated by checkpoint kinases Chk1 and Chk2. *Genes Dev* 2004; **18**: 3041–54.
39 Zaika A, Irwin M, Sansome C, Moll UM. Oncogenes induce and activate endogenous p73 protein. *J Biol Chem* 2001; **276**: 11310–6.
40 Corn PG, Kuerbitz SJ, van Noesel MM *et al.* Transcriptional silencing of the p73 gene in acute lymphoblastic leukemia and Burkitt's lymphoma is associated with 5′ CpG island methylation. *Cancer Res* 1999; **59**: 3352–6.
41 Kawano S, Miller CW, Gombart AF *et al.* Loss of p73 gene expression in leukemias/lymphomas due to hypermethylation. *Blood* 1999; **94**: 1113–20.
42 Banelli B, Casciano I, Romani M. Methylation-independent silencing of the p73 gene in neuroblastoma. *Oncogene* 2000; **19**: 4553–6.
43 Nomoto S, Haruki N, Kondo M *et al.* Search for mutations and examination of allelic expression imbalance of the p73 gene at 1p36.33 in human lung cancers. *Cancer Res* 1998; **58**: 1380–3.
44 Takahashi T, Ichimiya S, Nimura Y *et al.* Mutation, allelotyping, and transcription analyses of the p73 gene in prostatic carcinoma. *Cancer Res* 1998; **58**: 2076–7.
45 Nimura Y, Mihara M, Ichimiya S *et al.* p73, a gene related to p53, is not mutated in esophageal carcinomas. *Int J Cancer* 1998; **78**: 437–40.
46 Ichimiya S, Nimura Y, Kageyama H *et al.* p73 at chromosome 1p36.3 is lost in advanced stage neuroblastoma but its mutation is infrequent. *Oncogene* 1999; **18**: 1061–6.
47 Mihara M, Nimura Y, Ichimiya S *et al.* Absence of mutation of the p73 gene localized at chromosome 1p36.3 in hepatocellular carcinoma. *Br J Cancer* 1999; **79**: 164–7.
48 Shishikura T, Ichimiya S, Ozaki T *et al.* Mutational analysis of the p73 gene in human breast cancers. *Int J Cancer* 1999; **84**: 321–5.
49 Takada N, Ozaki T, Ichimiya S, Todo S, Nakagawara A. Identification of a transactivation activity in the COOH-terminal region of p73 which is impaired in the naturally occurring mutants found in human neuroblastomas. *Cancer Res* 1999; **59**: 2810–4.
50 Naka M, Ozaki T, Takada N *et al.* Functional characterization of naturally occurring mutants (P405R and P425L) of p73α and p73β found in neuroblastoma and lung cancer. *Oncogene* 2001; **20**: 3568–72.

 doi: 10.1111/j.1349-7006.2005.00116.x

51 Donehower LA, Harvey BL, Slagle BL *et al.* Mice deficient for p53 are developmentally normal but susceptible to spontaneous tumours. *Nature* 1992; **356**: 215–21.
52 Gong J, Constanzo A, Yang H-Q *et al.* The tyrosine kinase c-Abl regulates p73 in apoptotic response to cisplatin-induced DNA damage. *Nature* 1999; **399**: 806–9.
53 Agami R, Blandino G, Oren M, Shaul Y. Interaction of c-Abl and p73α and their collaboration to induce apoptosis. *Nature* 1999; **399**: 809–13.
54 Yuan Z-M, Shioya H, Ishiko T *et al.* p73 is regulated by tyrosine kinase c-Abl in the apoptotic response to DNA damage. *Nature* 1999; **399**: 814–7.
55 Ren J, Datta R, Shioya H *et al.* p73β is regulated by protein kinase Cδ catalytic fragment generated in the apoptotic response to DNA damage. *J Biol Chem* 2002; **277**: 33758–65.
56 Gonzalez S, Prives C, Cordon-Cardo C. p73α regulation by Chk1 in response to DNA damage. *Mol Cell Biol* 2003; **23**: 8161–71.
57 Gaiddon C, Lokshin M, Gross I *et al.* Cyclin-dependent kinases phosphorylate p73 at threonine 86 in a cell cycle-dependent manner and negatively regulate p73. *J Biol Chem* 2003; **278**: 27421–31.
58 Zeng X, Li X, Miller A *et al.* The N-terminal domain of p73 interacts with the CH1 domain of p300/CREB binding protein and mediates transcriptional activation and apoptosis. *Mol Cell Biol* 2000; **20**: 1299–310.
59 Costanzo A, Merlo P, Pediconi N *et al.* DNA damage-dependent acetylation of p73 dictates the selective activation of apoptotic target genes. *Mol Cell* 2002; **9**: 175–86.
60 Mantovani F, Piazza S, Gostissa M *et al.* Pin1 links the activities of c-Abl and p300 in regulating p73 function. *Mol Cell* 2004; **14**: 625–36.
61 Kramer S, Ozaki T, Miyazaki K, Kato C, Hanamoto T, Nakagawara A. Protein stability and function of p73 are modulated by a physical interaction with RanBPM in mammalian cultured cells. *Oncogene* 2005; **24**: 938–44.
62 Leng RP, Lin Y, Ma W *et al.* Pirh2, a p53-induced ubiquitin protein ligase, promotes p53 degradation. *Cell* 2003; **112**: 779–91.
63 Wu L, Zhu H, Nie L, Maki CG. A link between p73 transcriptional activity and p73 degradation. *Oncogene* 2004; **23**: 4032–6.
64 Rossi M, De Laurenzi V, Munarriz E *et al.* The ubiquitin-protein ligase Itch regulates p73 stability. *EMBO J* 2005; **24**: 836–48.
65 Miyazaki K, Ozaki T, Kato C *et al.* A novel HECT-type E3 ubiquitin ligase, NEDL2, stabilizes p73 and enhances its transcriptional activity. *Biochem Biophys Res Commun* 2003; **308**: 106–13.
66 Toh WH, Siddique MM, Boominathan L, Lin KW, Sabapathy K. c-Jun regulates the stability and activity of the p53 homologue, p73. *J Biol Chem* 2004; **279**: 44713–22.
67 Hosoda M, Ozaki T, Miyazaki K *et al.* UFD2a mediates the proteasomal turnover without promoting p73 ubiquitination. *Oncogene* (forthcoming).
68 Marin MC, Jost CA, Irwin MS *et al.* Viral oncoproteins discriminate between p53 and the p53 homolog p73. *Mol Cell Biol* 1998; **18**: 6316–24.
69 Roth J, Konig C, Wienzek S *et al.* Inactivation of p53 but not p73 by adenovirus type 5 E1B 55-kilodalton and E4 34-kilodalton oncoproteins. *J Virol* 1998; **72**: 8510–6.
70 Steegenga WT, Shvarts A, Riteco N, Bos JL, Jochemsen AG. Distinct regulation of p53 and p73 activity by adenovirus E1A, E1B, and E4orf6 proteins. *Mol Cell Biol* 1999; **19**: 3885–94.
71 Dobbelstein M, Wienzek S, Konig C, Roth J. Inactivation of the p53-homologue p73 by the MDM2-oncoprotein. *Oncogene* 1999; **18**: 2101–6.
72 Strano S, Munarriz E, Rossi M *et al.* Physical interaction with Yes-associated protein enhances p73 transcriptional activity. *J Biol Chem* 2001; **276**: 15164–73.
73 Watanabe K, Ozaki T, Nakagawa T *et al.* Physical interaction of p73 with c-Myc and MM1, a c-Myc-binding protein, and modulation of the p73 function. *J Biol Chem* 2002; **277**: 15113–23.
74 Ozaki T, Watanabe K, Nakagawa T *et al.* Function of p73, but not of p53, is inhibited by the physical interaction with RACK1 and its inhibitory effect is counteracted by pRB. *Oncogene* 2003; **22**: 3231–42.
75 Hanamoto T, Ozaki T, Furuya K *et al.* Identification of protein kinase A catalytic subunit β as a novel binding partner of p73 and regulation of p73 function. *J Biol Chem* 2005; **280**: 16665–75.
76 Di Como CJ, Gaiddon C, Prives C. p73 function is inhibited by tumor-derived p53 mutants in mammalian cells. *Mol Cell Biol* 1999; **19**: 1438–49.
77 Marin MC, Jost CA, Brooks LA *et al.* A common polymorphysm acts as intragenic modifier of mutant p53 behaviour. *Nat Genet* 2000; **25**: 47–54.
78 Bergamaschi D, Gasco M, Hiller L *et al.* p53 polymorphysm influences response in cancer chemotherapy via modulation of p73-dependent apoptosis. *Cancer Cell* 2003; **3**: 387–402.
79 Miro-Mur F, Meiller A, Haddada H, May E. p73α expression induces both accumulation and activation of wt-p53 independent of the p73α transcriptional activity. *Oncogene* 2003; **22**: 5451–6.
80 Goldschneider D, Blanc E, Raguenez G *et al.* When p53 needs p73 to be functional-forced p73 expression induces nuclear accumulation of endogenous p53 protein. *Cancer Lett* 2003; **197**: 99–103.
81 Vikhanskaya F, D'Incalci M, Broggini M. p73 competes with p53 and attenuates its response in a human ovarian cancer cell line. *Nucl Acids Res* 2000; **28**: 513–9.
82 Billon N, Terrinoni A, Jolicoeur C *et al.* Roles for p53 and p73 during oligodendrocyte development. *Development* 2004; **131**: 1211–20.
83 Rodicker F, Putzer BM. p73 is effective in p53-null pancreatic cancer cells resistant to wild-type TP53 gene replacement. *Cancer Res* 2003; **63**: 2737–41.
84 Waltermann A, Kartasheva NN, Dobbelstein M. Differential regulation of p63 and p73 expression. *Oncogene* 2003; **22**: 5686–93.
85 Strano S, Rossi M, Fontemaggi G *et al.* From p63 to p53 across p73. *FEBS Lett* 2001; **490**: 163–70.
86 Mills AA, Zheng B, Wang X-J, Vogel H, Roop DR, Bradley A. p63 is a p53 homologue required for limb and epidermal morphogenesis. *Nature* 1999; **398**: 708–13.
87 Yang A, Schweitzer R, Sun D *et al.* p63 is essential for regenerative proliferation in limb, craniofacial and epithelial development. *Nature* 1999; **398**: 714–8.
88 Celli J, Duijf P, Hamel BCJ *et al.* Heterozygous germline mutations in the p53 homolog p63 are the cause of EEC syndrome. *Cell* 1999; **99**: 143–53.